# The Mu2e Muon Beamline

Rick Coleman

Fermilab

NuFact09/Muon Physics

20-25 July 2009

**LETTERS TO THE EDITOR**

**On the search for the $\mu \rightarrow e$ conversion process in a nucleus**

R. M. Dzhilkibaev and V. M. Lobashev

*Institute of Nuclear Research, USSR Academy of Sciences*

(Submitted 21 June 1988)
Yad. Fiz. **49**, 622–624 (February 1989)

## $\mu/p \sim 10^{-4}$ vs conventional $\sim 10^{-8}$

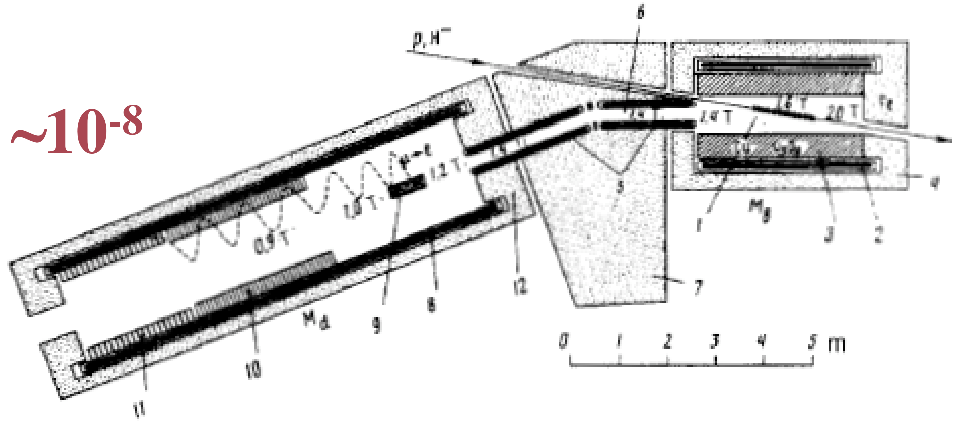


# MECO

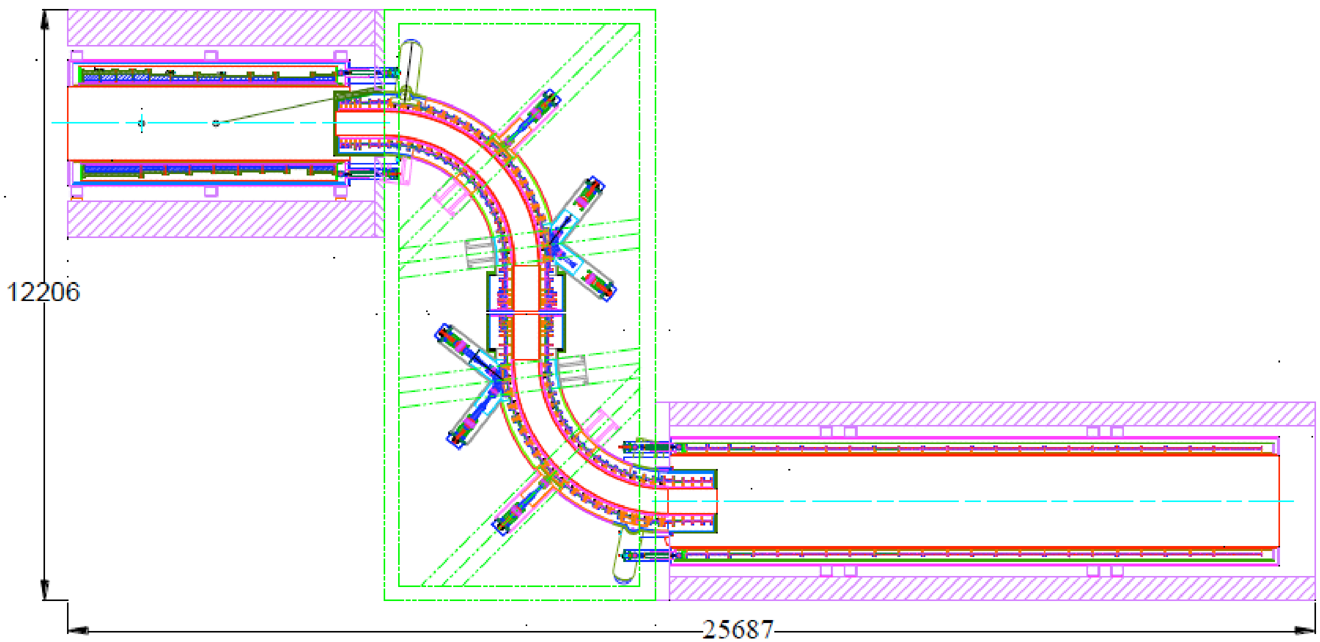

Muons are collected, transported, and detected in solenoidal magnets

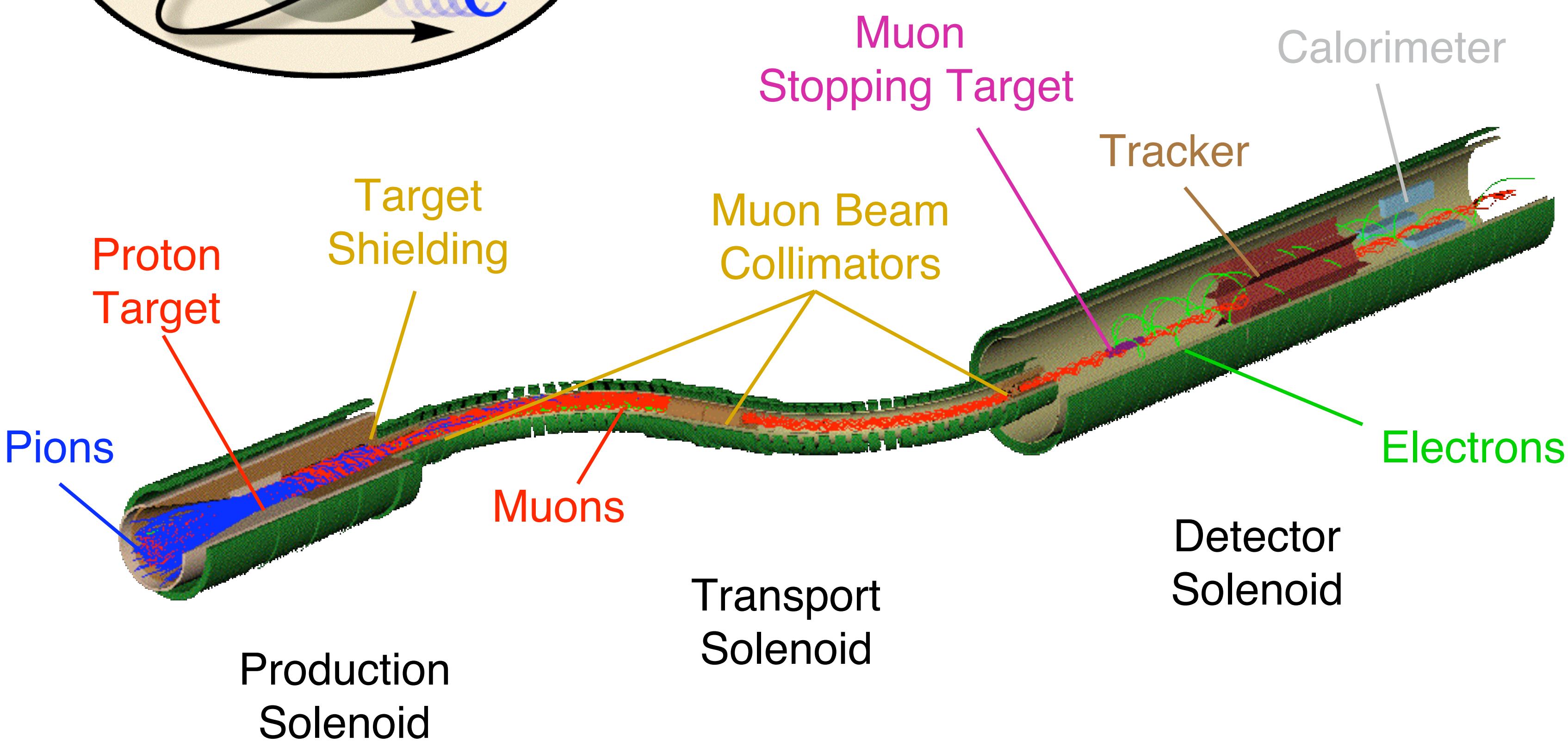


# Mu2e Muon Beamline- follows MECO design

more information at http://mu2e.fnal.gov

# Muon Beamline Requirements

- Deliver high flux $\mu^-$ beam to stopping target
  - high proton flux 2 x $10^{13}$ /sec
  - ~5 x $10^{10}$ Hz $\mu^-$ , $10^{18}$ total, 4 conversion $e^-$ at $R_{\mu e}$~$10^{-16}$
- Pulsed beam - Wait for background particles from proton beam hitting target to subside, then look for conversion $e^-$

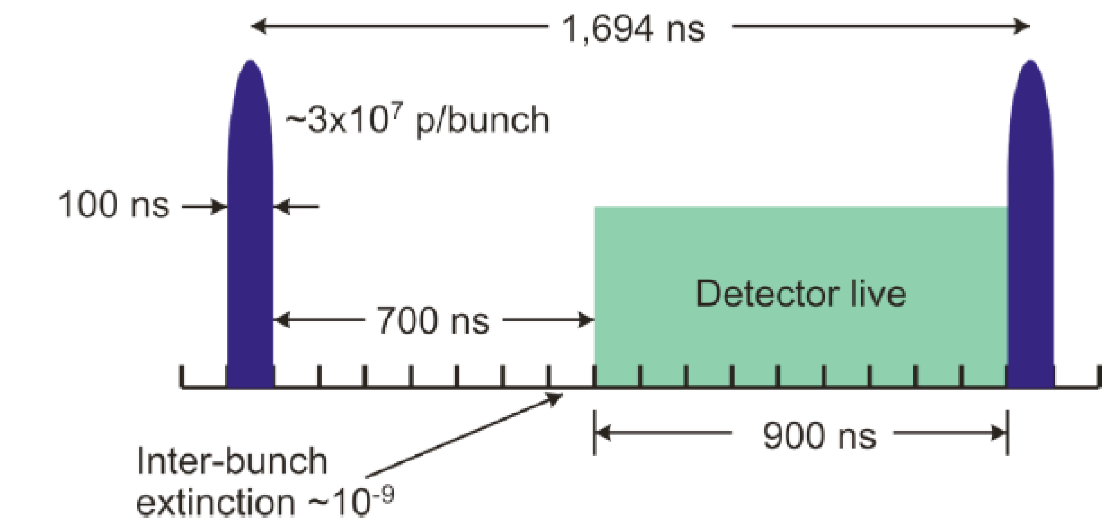


$\tau_{\mu}$(Al)=864 ns

Other Mu2e talks at this workshop: Doug Glenzinski- Mu2e project,
Mike Sypher's talk on Accelerator issues, Eric Prebys' talk on Proton Extinction

# Muon Beamline Requirements (continued)

- Muon properties
  - low energies
    - stop max # muons in thin target
    - backgrounds
  - small beam spot to minimize target radius

- Background particles from beamline must be minimized
- a major force driving design of the muon beamline
  - especially ~105 MeV $e^-$
  - Radiative pion capture in stopping target $\pi^- + (A,Z) \rightarrow (A',Z') + X + \gamma$
  - Decays with late arriving electrons

$$\pi^- \rightarrow e^- + \overline{\nu}_e \ (p > 55 \text{ MeV/c}), \quad \mu^- \rightarrow e^- + \overline{\nu}_e + \nu_\mu \ (p > 75 \text{ MeV/c})$$

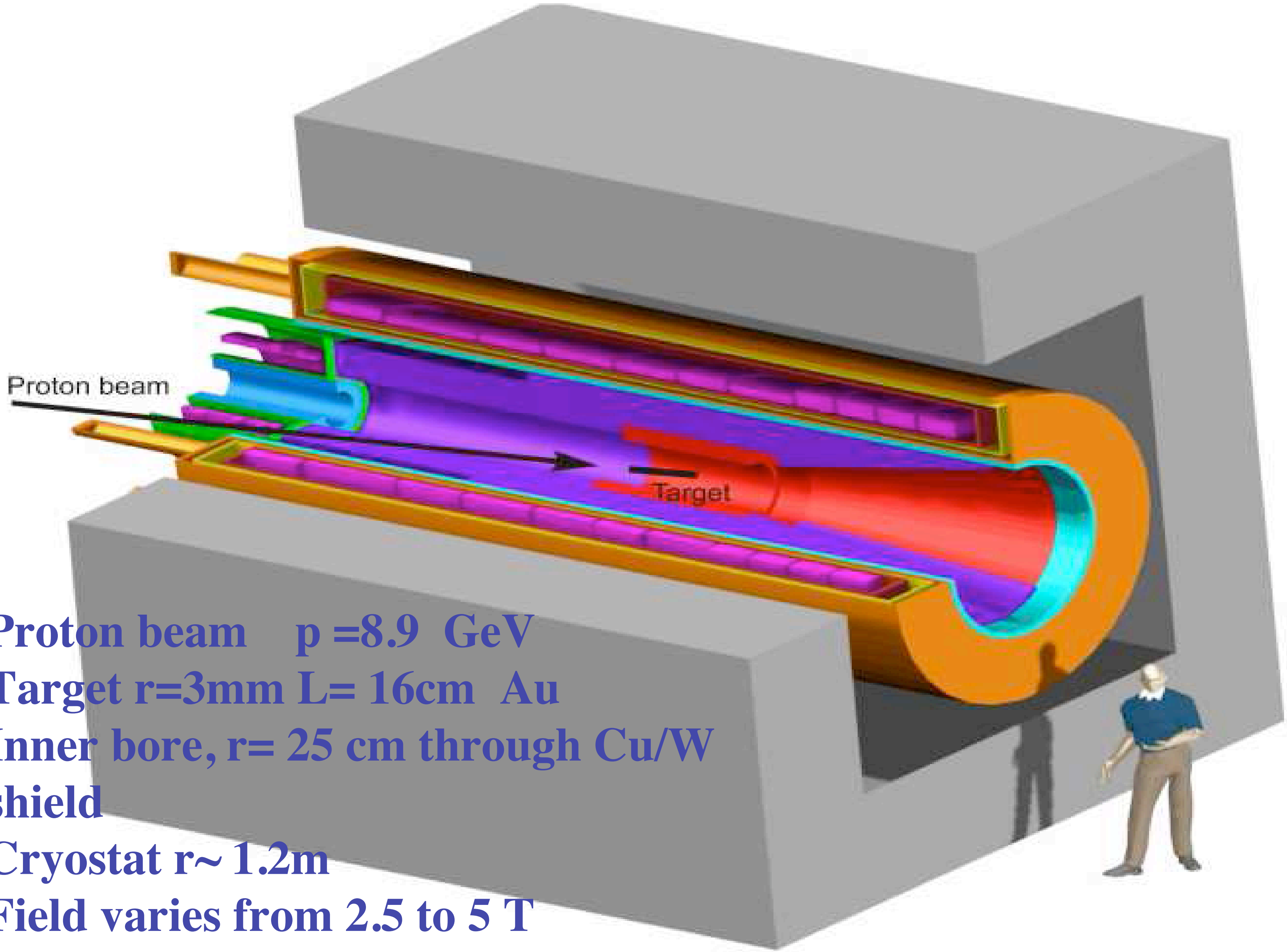


**Proton beam p =8.9 GeV**
**Target r=3mm L= 16cm Au**
**Inner bore, r= 25 cm through Cu/W shield**
**Cryostat r~ 1.2m**
**Field varies from 2.5 to 5 T**

# *MECO HEAT/RADIATION PRODUCTION SOLENOID*

MECO beam power 50kW
(Mu2e ~2x less)

**Target** 7 kW

**Shield** 16 kW
both water-cooled

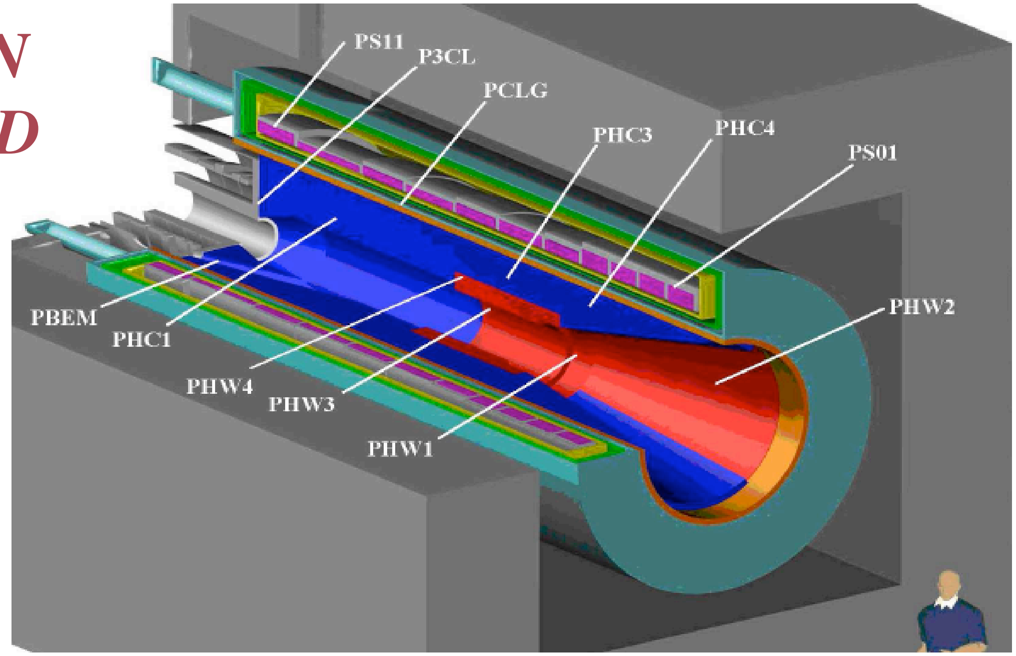


*Figure 7.11: Cutaway view of the heat and radiation shield within the warm bore of the Production Solenoid. In the figure, copper is blue and tungsten is red, while the stainless steel volumes are in several colors to distinguish regions.*

## Superconducting Coils

Local Maximum Instantaneous Power = 21 uW/gm
Maximum Total Power ~ 60 W
Maximum Dose any coil ~30 MRad

Absorber thickness at target of 45 cm W/Cu

*Table 7.2: Estimated steady state radiation heat loads*

| Volume | Power (W) |
|---|---|
| PHC1 | 1200 |
| PHC3 | 720 |
| PHC4 | 100 |
| PHW1 | 2700 |
| PHW2 | 1500 |
| PHW3 | 6200 |
| P3CL | 2000 |
| PCLG | 300 |
| PCIW | 41 |
| Total: | 15,741 |

# Pion Production- what energies and angles are important?

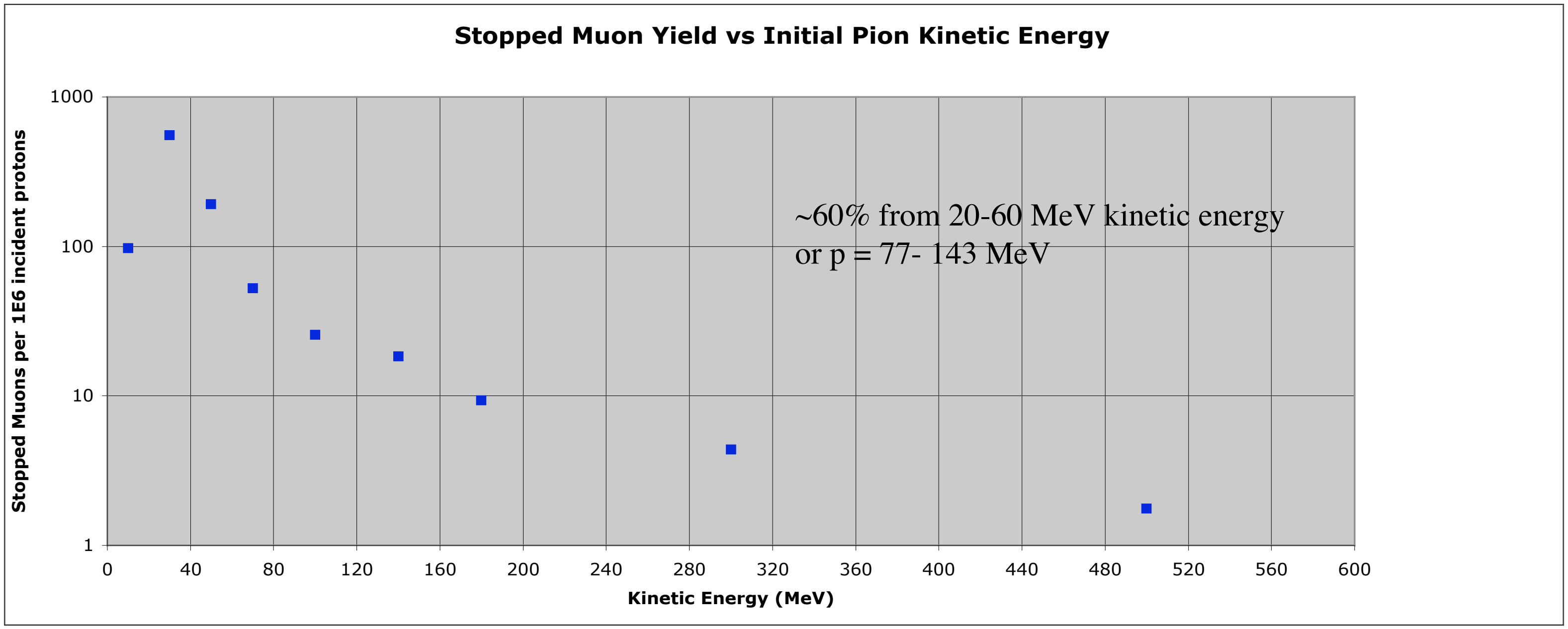


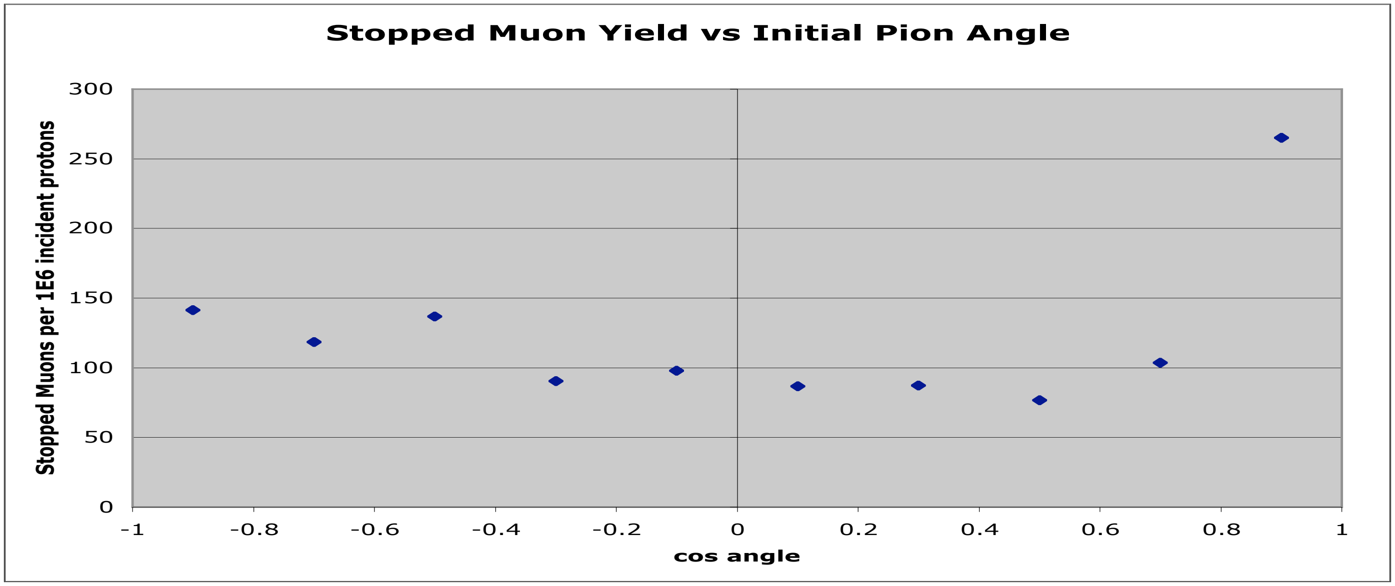

# $\pi^-$ Production- a work in progress

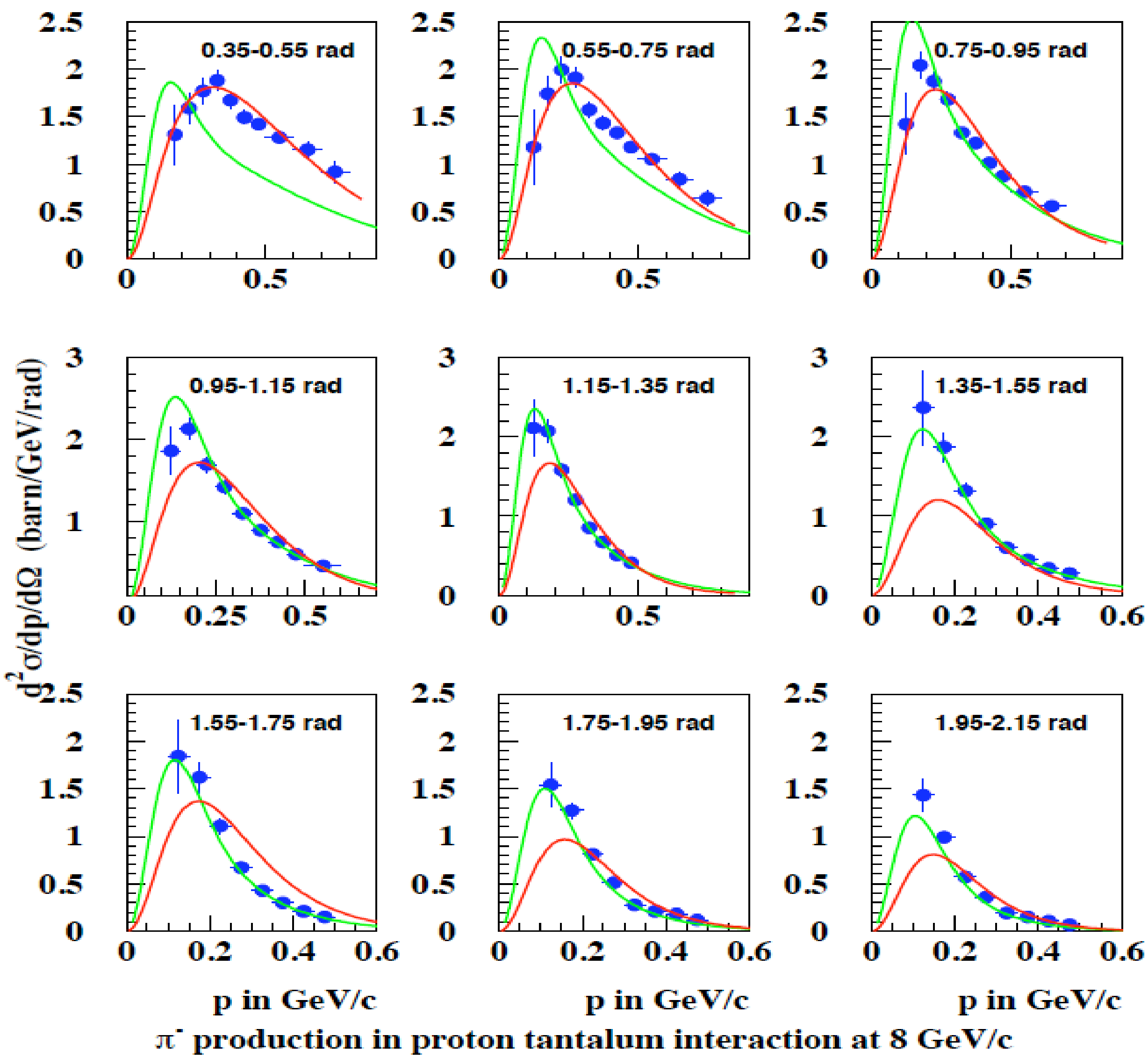


- HARP data

-Mu2e fit

-FANCY data* Striganov fit

•Pion yield was measured by FANCY spectrometer at KEK for p Al at 3 GeV/c and p Al, p Pb at 4 GeV/c Phys. Lett B B159;1,1985

# Study of Pion Production Data Used by MECO

10 GeV p + Ta -> $\pi^-$ + X    Thin Ta plates (1mm) in a bubble chamber

D. Artmutliski et al., Sov. J. Nucl. Phys. 48, 161 (1988), Prep. JINR P1-91-191 (1991).

**Original paper**

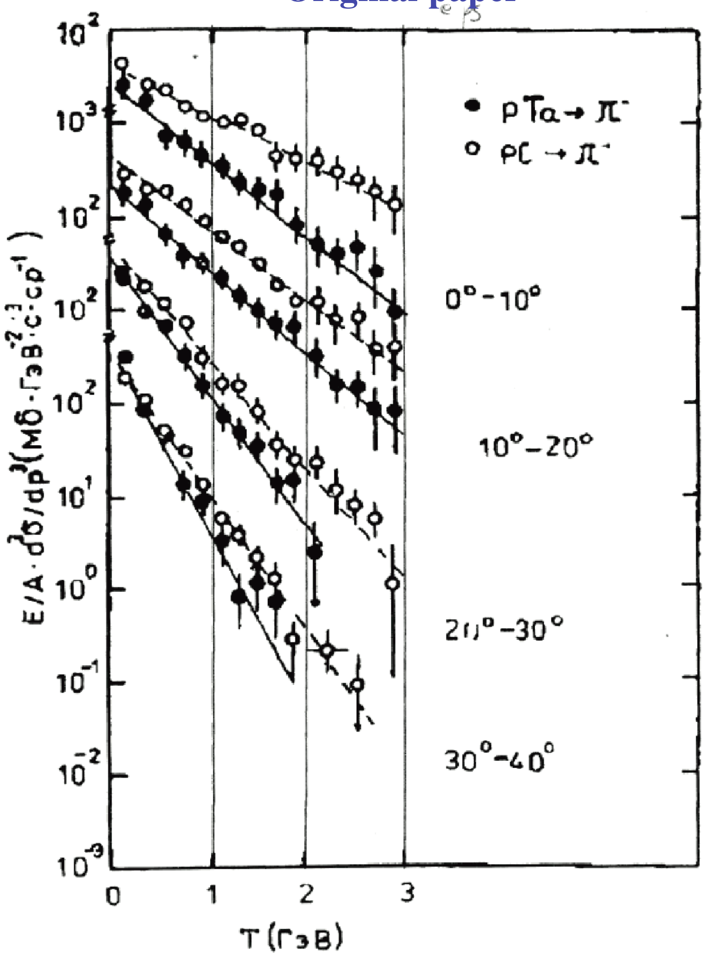


**MECO**

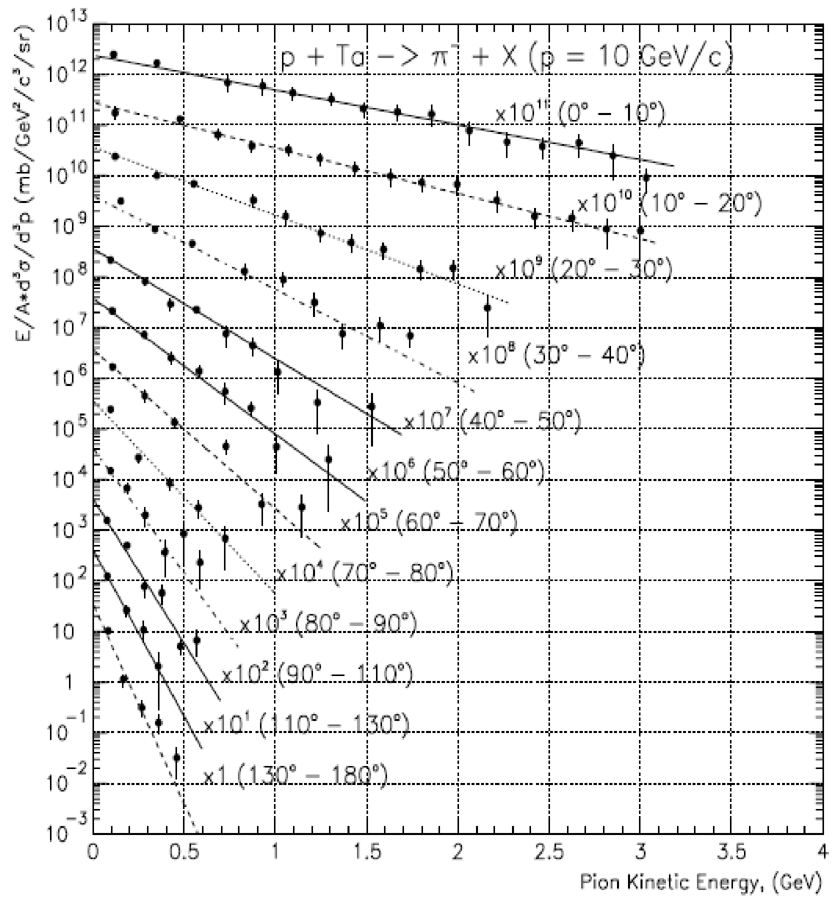


$$f = C \cdot \exp(-T/T_0)$$

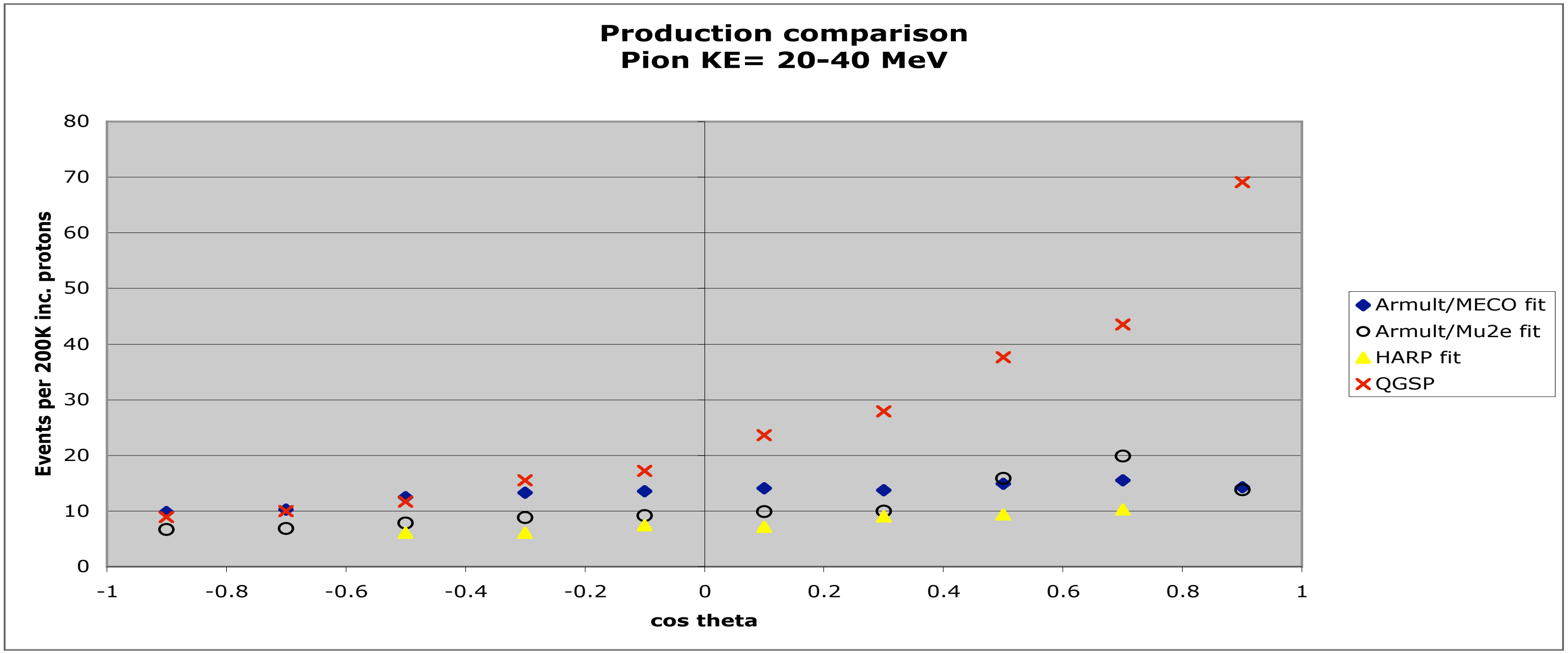

Production comparison
Pion KE= 20-40 MeV
Events per 200K inc. protons
cos theta
Armult/MECO fit
Armult/Mu2e fit
HARP fit
QGSP


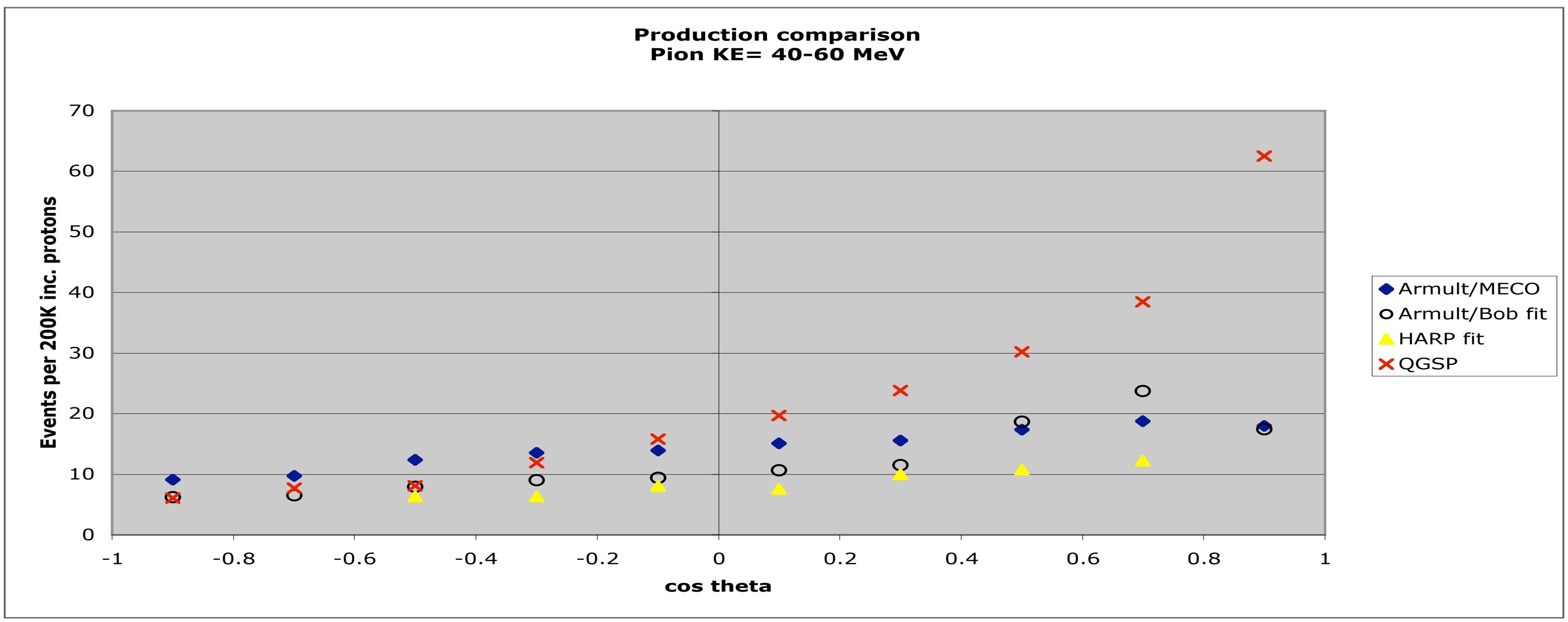

Production comparison
Pion KE= 40-60 MeV
Events per 200K inc. protons
cos theta
Armult/MECO
Armult/Bob fit
HARP fit
QGSP

# Transport Solenoid

Inner radius=25 cm
Length=13.11 m
TS1: L=1 m
TS2: R=2.9 m
TS3: L=2 m
TS4: R=2.9 m
TS5: L=1 m

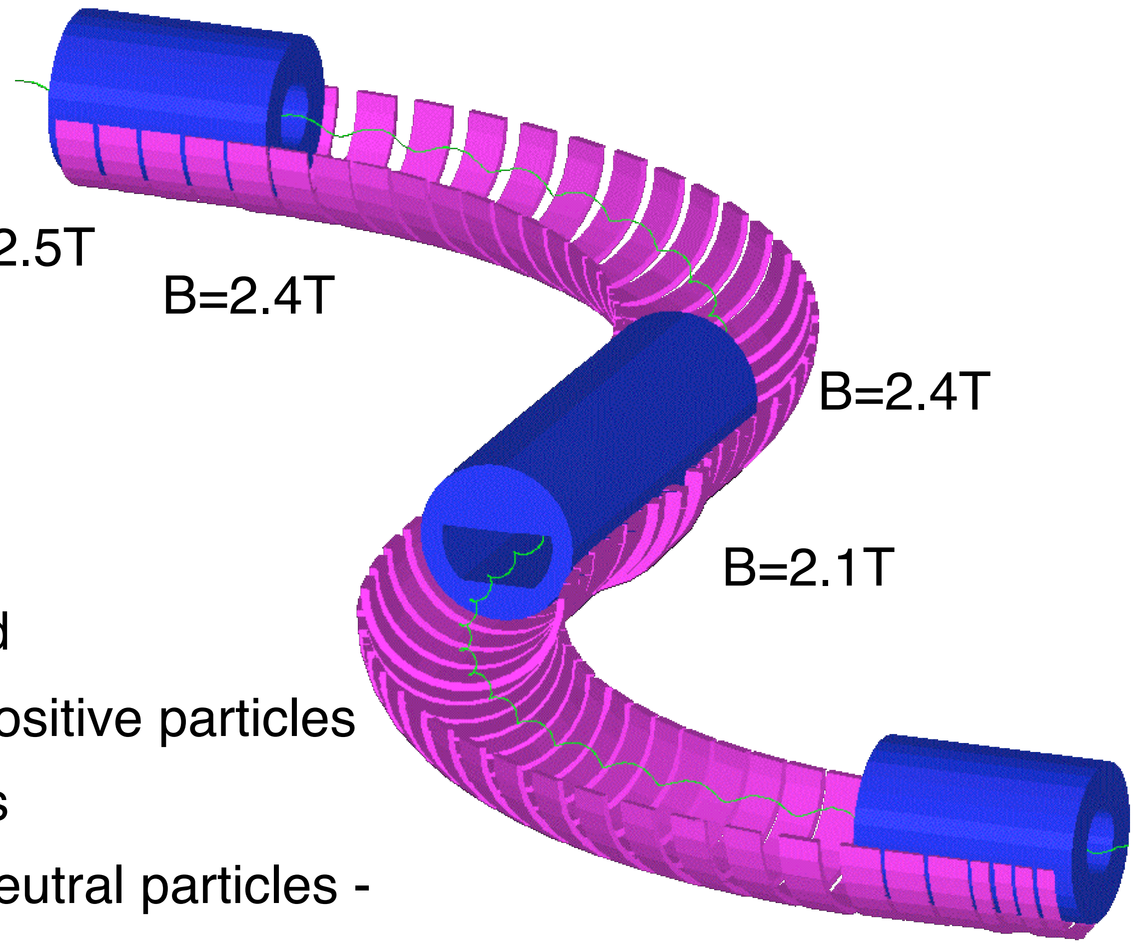


## Goals:

— Transport low energy $\mu^-$ to the detector solenoid

— Minimize transport of positive particles and high energy particles

— Minimize transport of neutral particles - curved section

— Absorb antiprotons in a thin window

— Minimize particles with long transit time

# Vertical Drift Motion in a Toroid

Toroidal Field: $B_s$=constant x 1/r. This gives a large $dB_s/dr$

Particle spiral drifts vertically (perpendicular to the plane of the toroid bend):

D= vertical drift distance

R=major toroid radius,

s/R = toroid angle=$90^0$

D[m]=distance, B[T], p[GeV/c]

$$\text{Define pitch } = \alpha = \frac{p_l}{p}$$

$$\rightarrow D = \frac{q}{0.3 \times B} \times \frac{s}{R} \times \frac{1}{2} p\left(\frac{1}{\alpha} + \alpha\right).$$

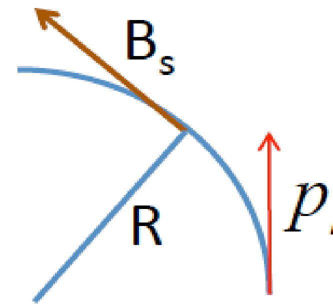


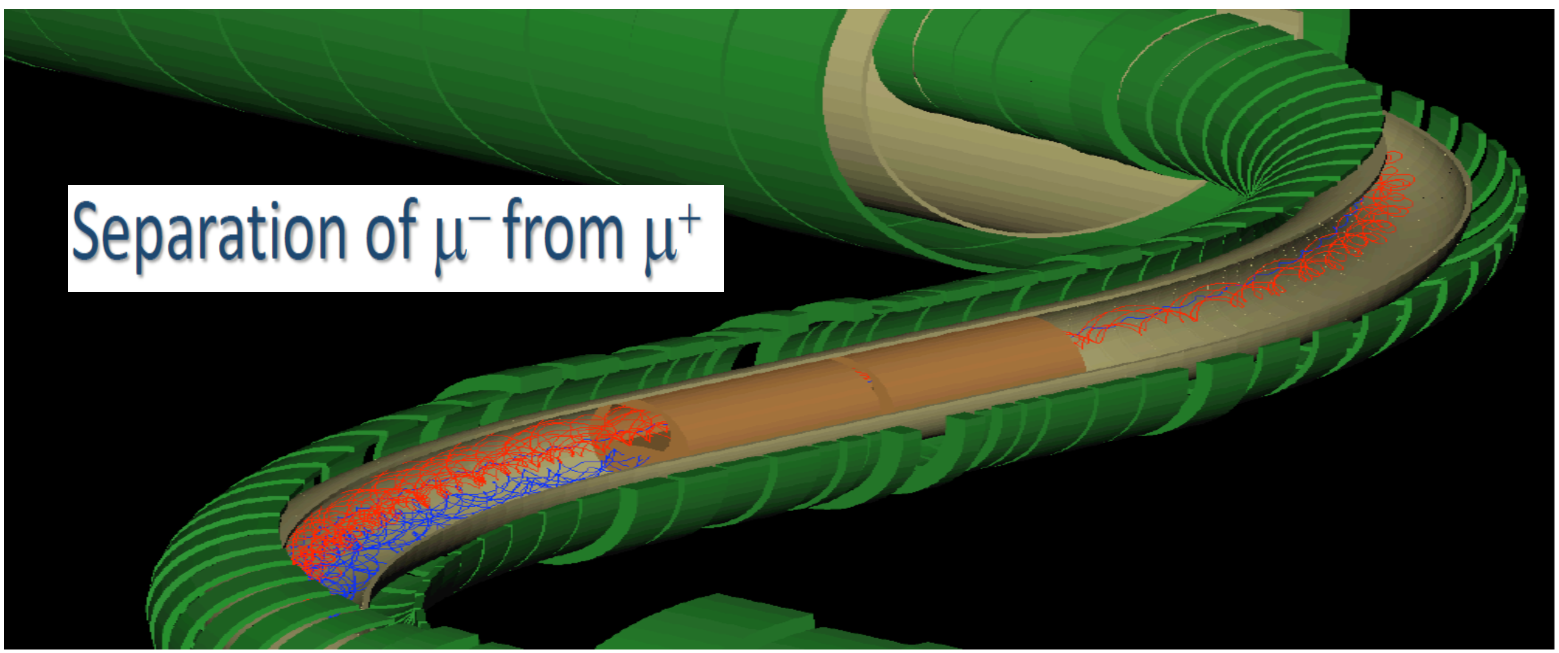

# For a given pitch, D depends linearly on momemtum

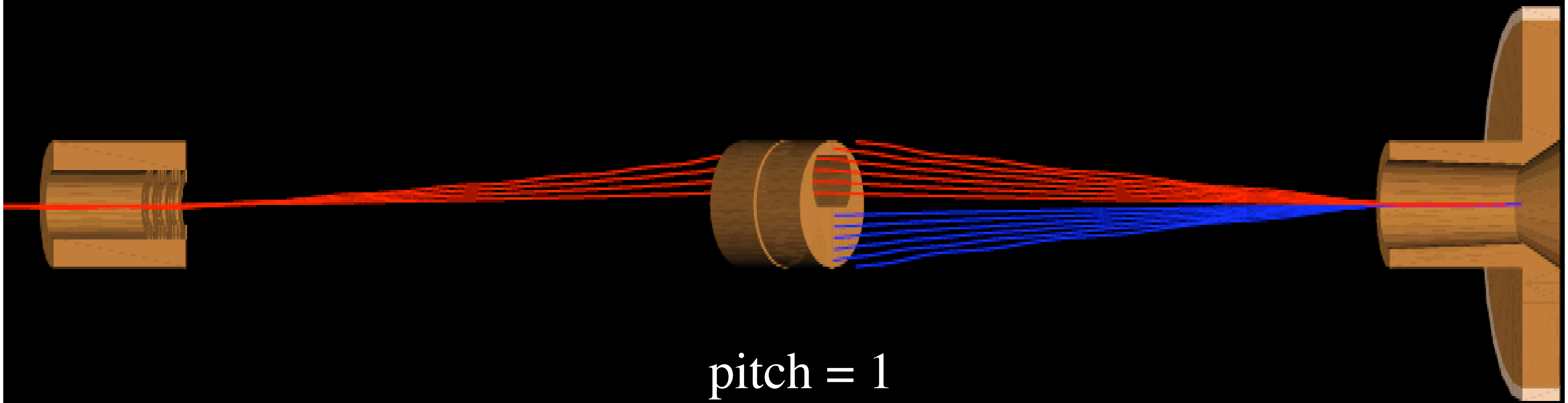

pitch = 1

p= 20,40,60,80,100,120 MeV

## As the pitch goes to zero, D becomes large

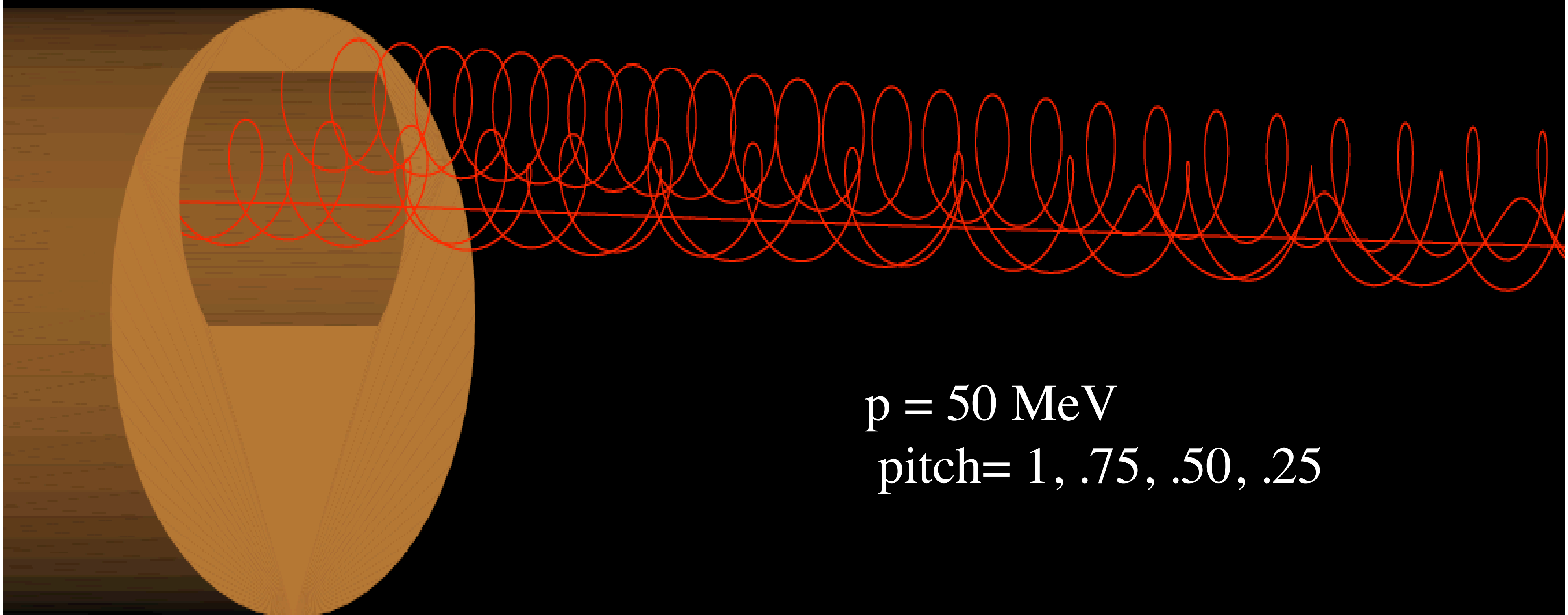


Slow-advancing particles (small pitch) get swept away

dBs/ds <0 can be relaxed

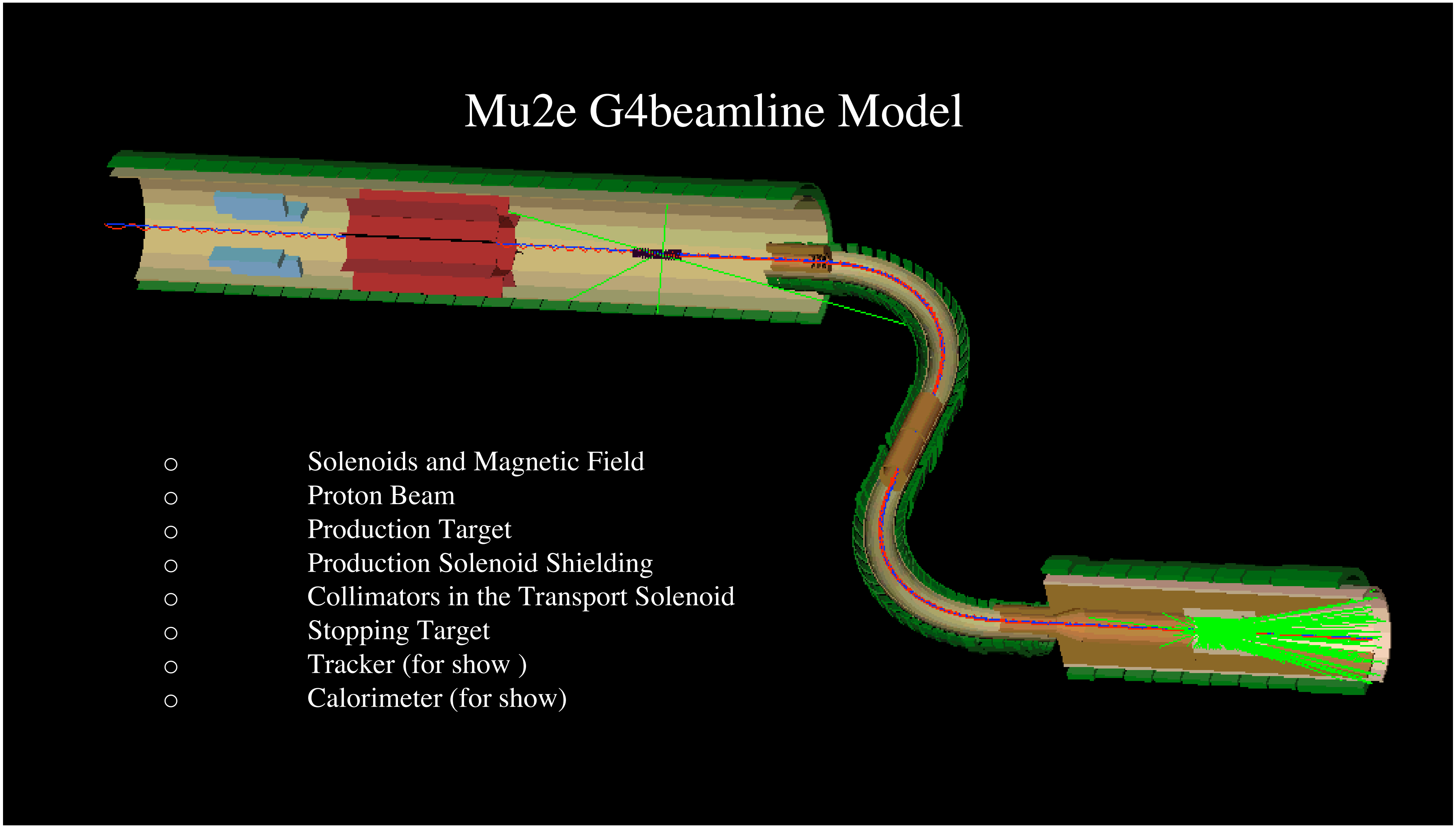


Mu2e Muon Beamline Simulation by Mike Martens 9/08

Thanks to Tom Roberts for much support on G4beamline

# Sampling of MECO simulations

- stopped muon / proton = 0.0022-.0025
- "Mirror" is 30% of muon yield
- PS r= 20-**25**-30 cm → 96-99.5-100%
- TS r=**15-10** cm → 100-56%
- Field max **5**-4.5-4.0T → 100-94-89%
- Water cooled target vs radiative <5%
- Proton beam angle 170 +/- 5 deg. → few %
- Target radius **3**-6mm → 100-65%
- Target L 12-**16**-20 cm ~ same
- Insensitive to small variation in target z



numbers in blue are design values

# Some Checks on Muon Yield

| | MECO | G4beamline |
|---|---|---|
| | | |
| Stopped muon yield per proton incident | 0.0022-0.0025 | 0.0022 |
| PS mirror removed | ~0.7 | 0.79 |
| PS bore radius 30 cm to 20 cm | 0.96 | 0.98 |
| Proton beam angle 12 - > 5 deg | 0.98 | 0.98 |
| Target radius 3 mm-> 6mm | 0.65 | 0.64 |
| Target L= 16 to 12 cm | 0.91 | 0.92 |
| Target L=16 to 20 | 0.99 | 0.96 |
| Target z position in PS | See next plot | |
| PS max field | See next plot | |
| | | |

# Target z position Study

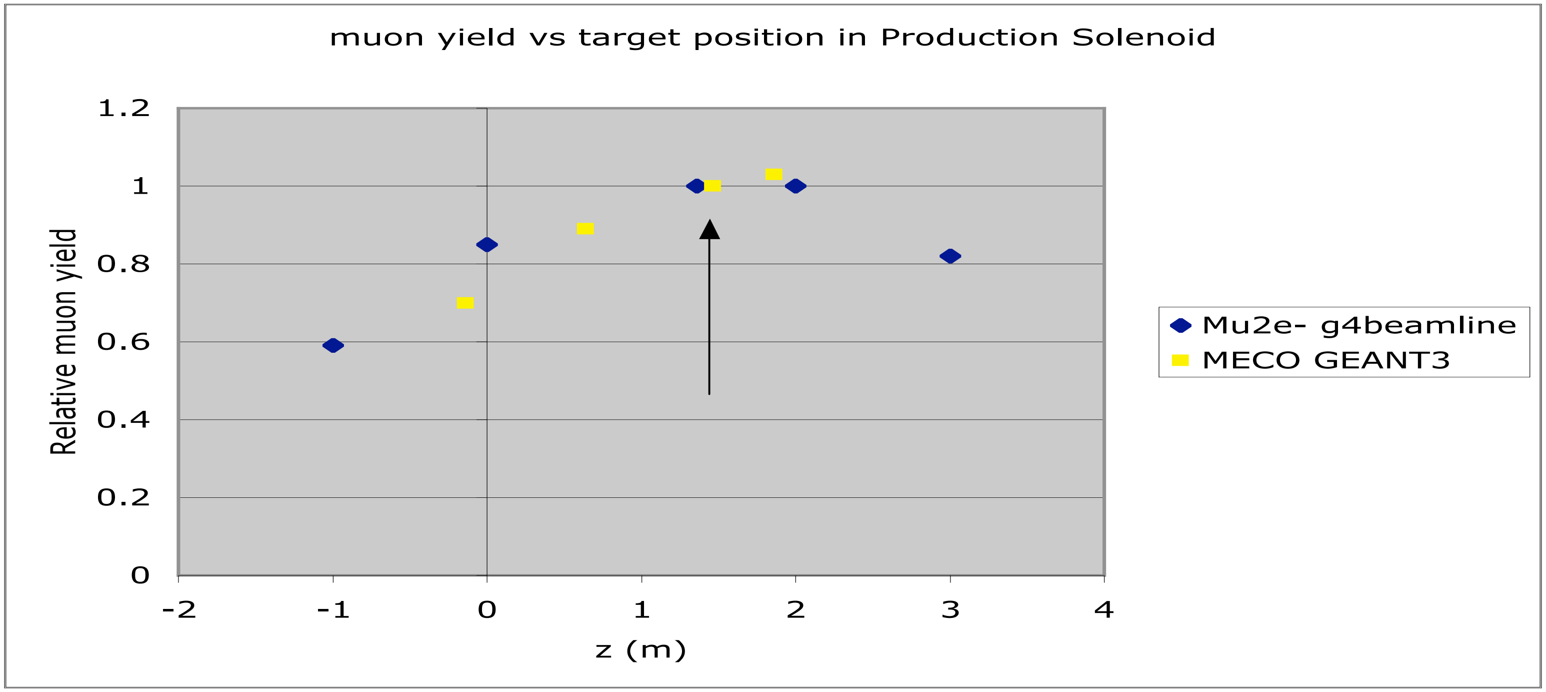


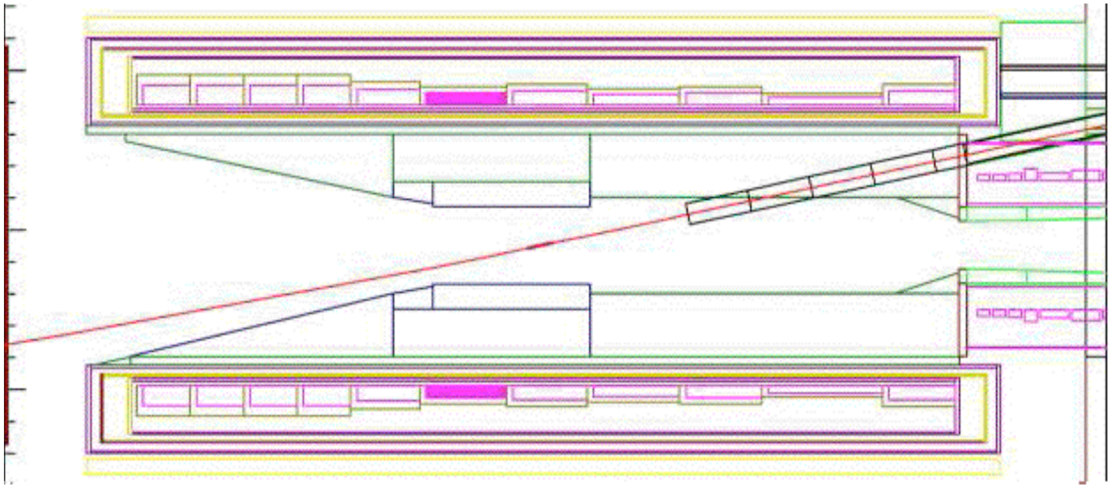

# Study of Muon Yield vs Maximum Field in Production Solenoid

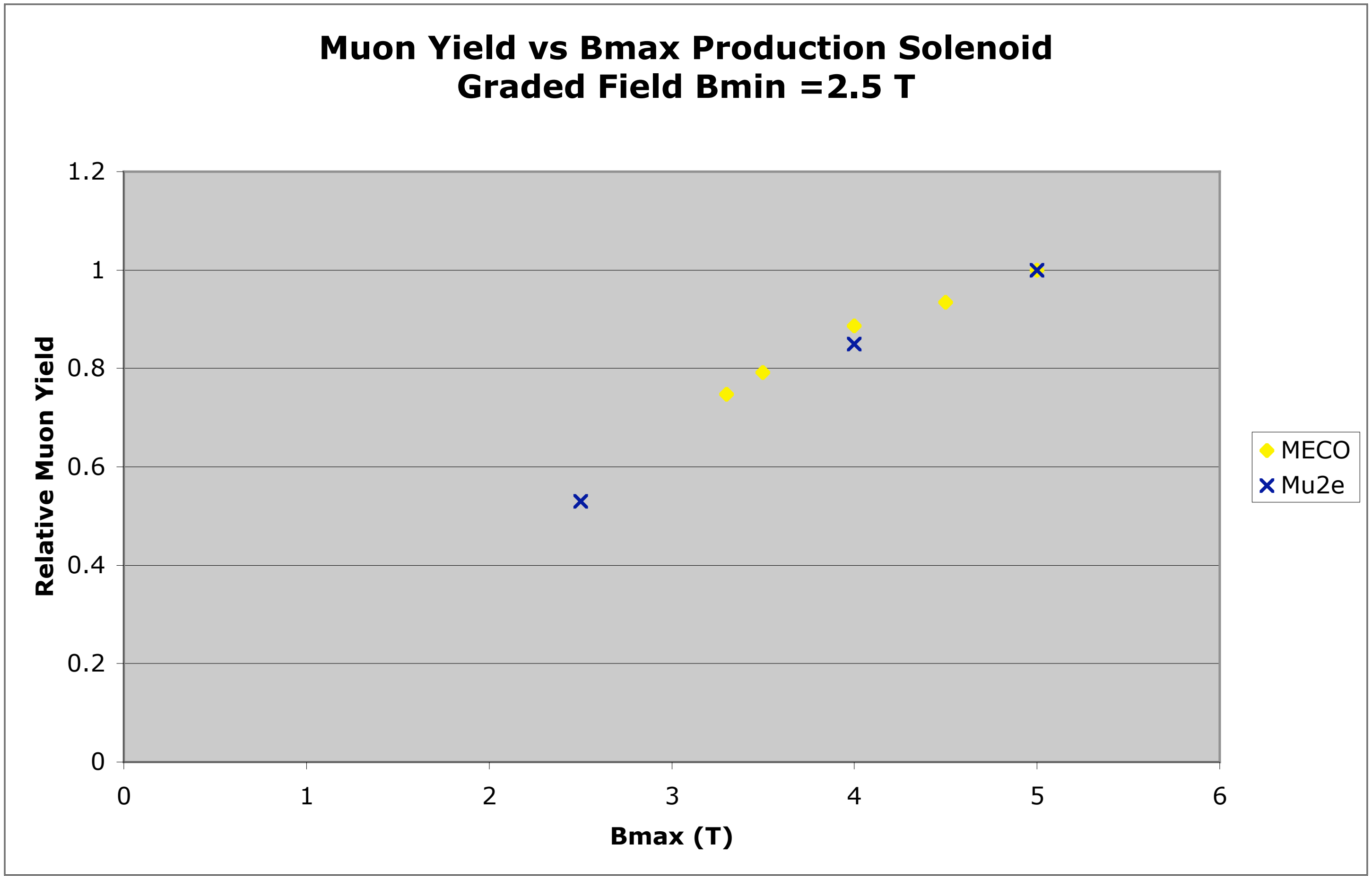

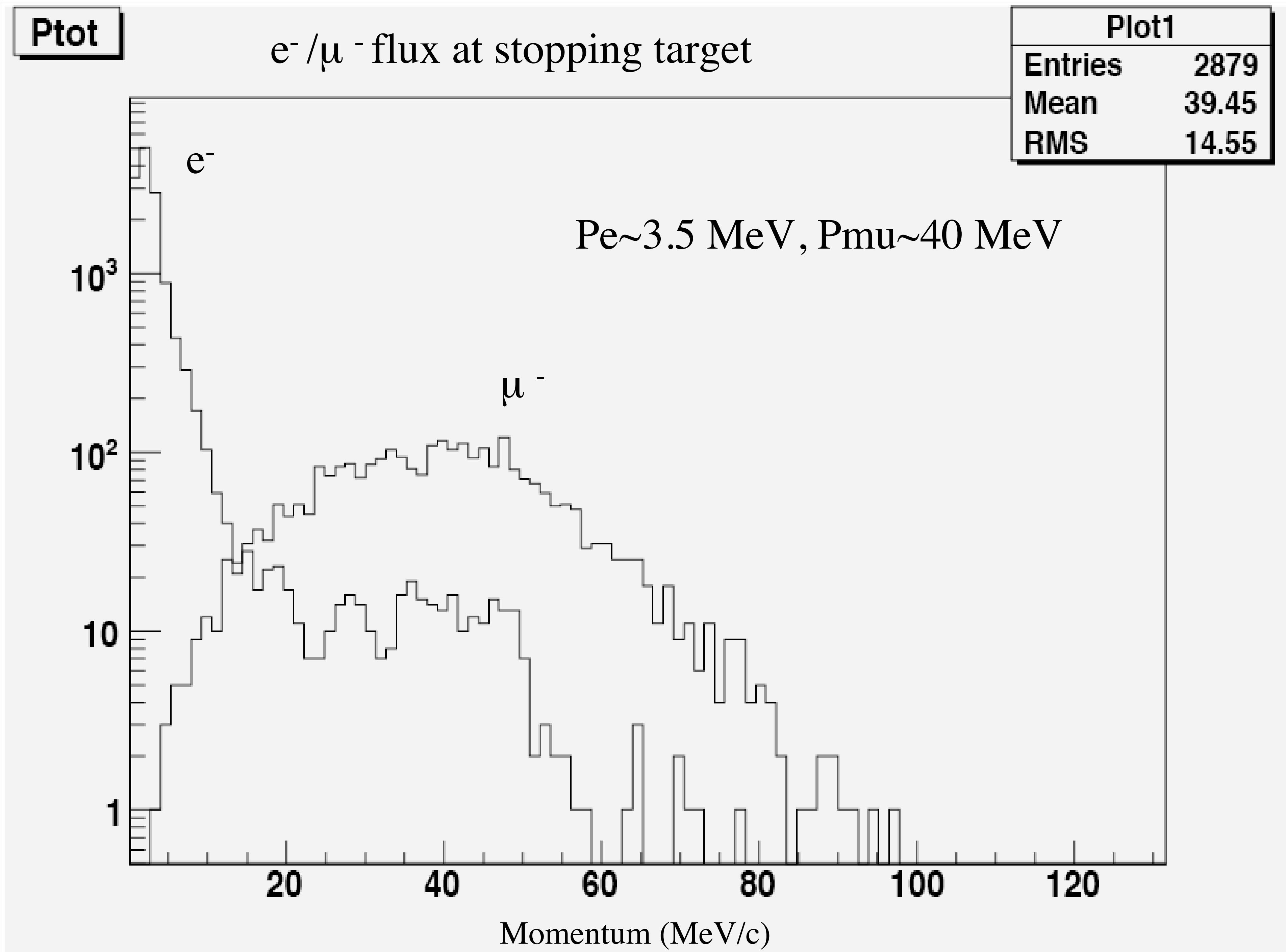

Ptot
e⁻/μ⁻ flux at stopping target
Plot1
Entries 2879
Mean 39.45
RMS 14.55
e⁻
Pe~3.5 MeV, Pmu~40 MeV
μ⁻
10³
10²
10
1
20
40
60
80
100
120
Momentum (MeV/c)

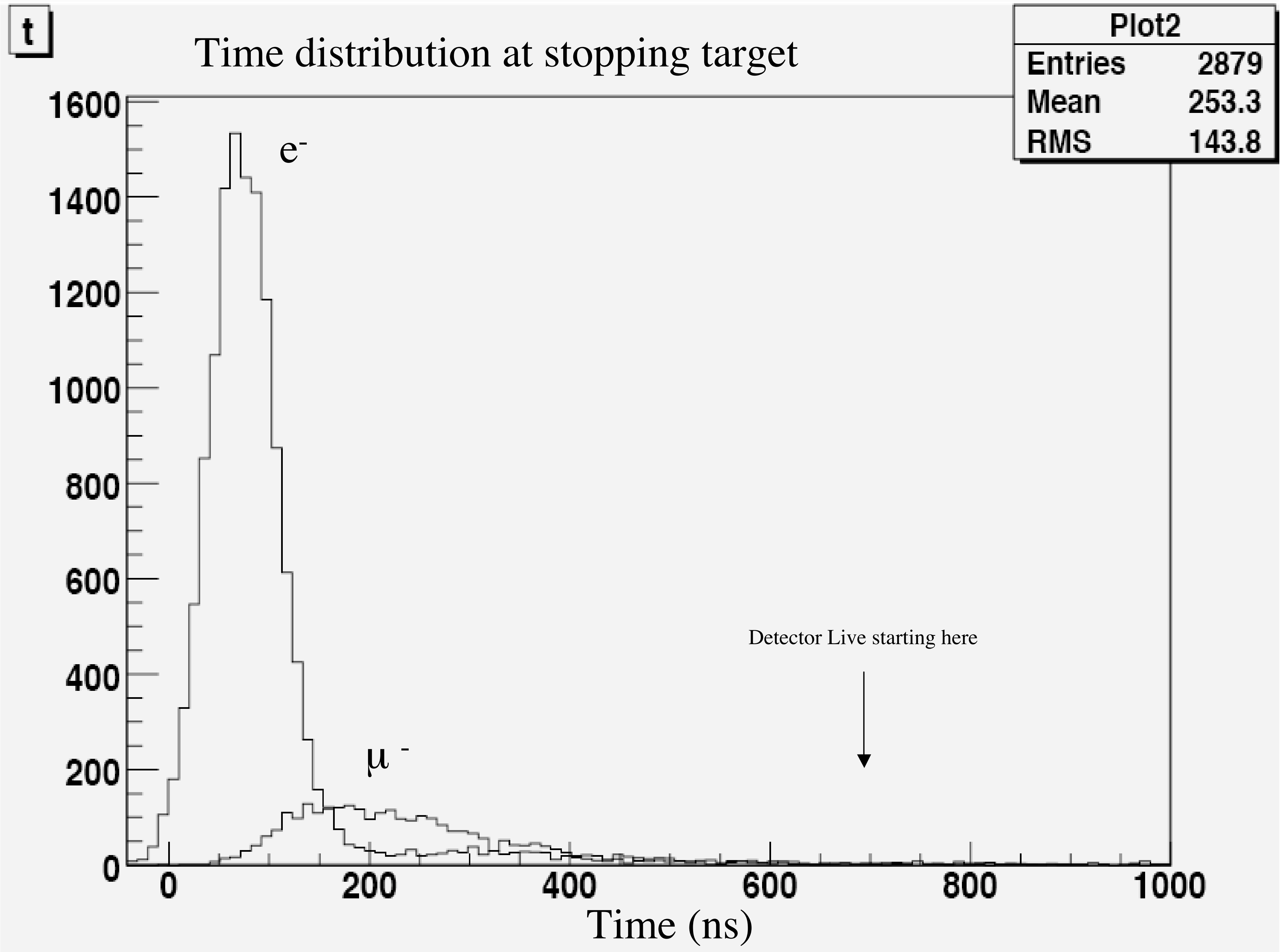
t
Time distribution at stopping target
Plot2
Entries 2879
Mean 253.3
RMS 143.8
e-
μ -
Detector Live starting here
1600
1400
1200
1000
800
600
400
200
0
0
200
400
600
800
1000
Time (ns)

Probability of $\pi^-$ reaching stopping target per proton

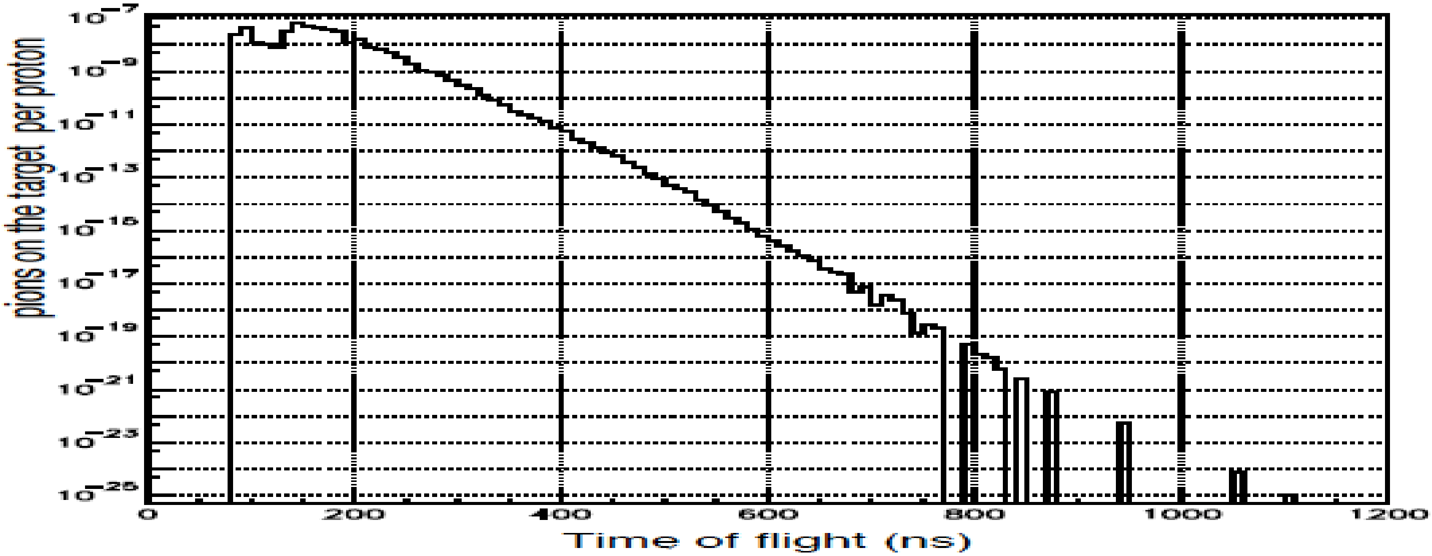


## MECO

$P_\pi$ (reaching stopping target)= 3 x $10^{-7}$

$P_\pi$(>700ns)= 4 x $10^{-18}$

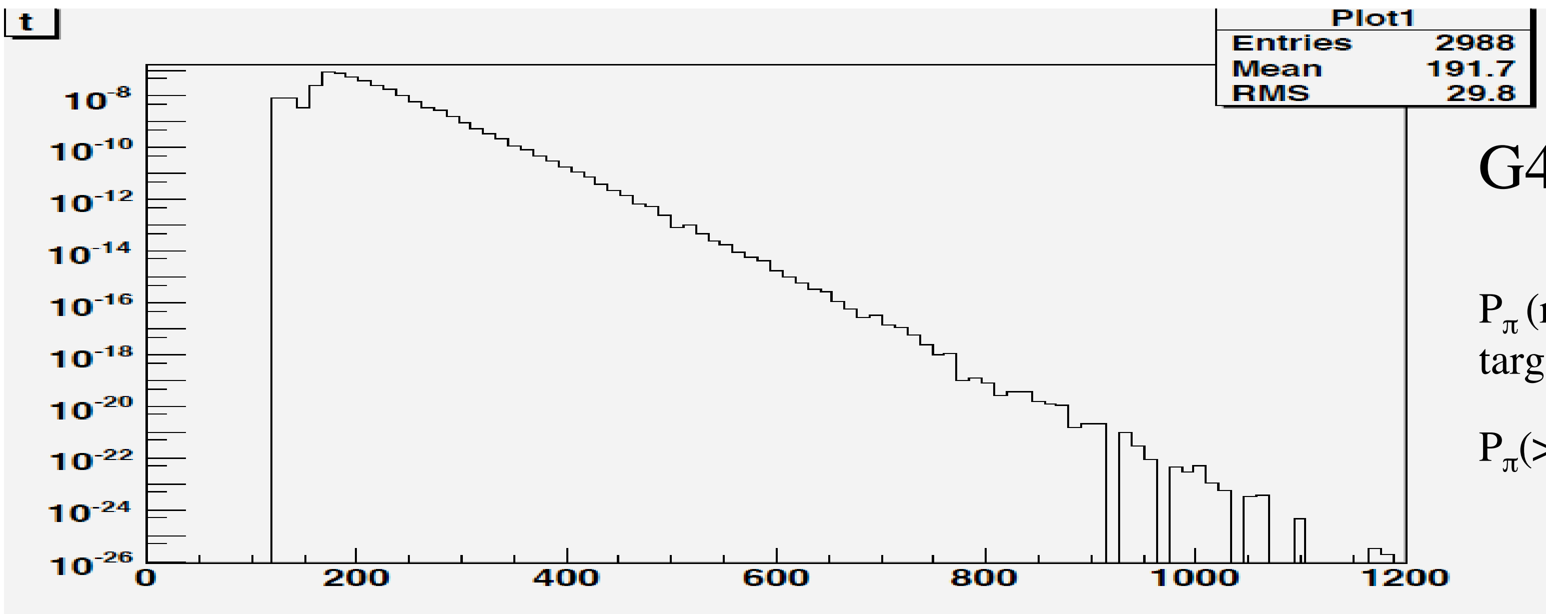


## G4beamline

$P_\pi$ (reaching stopping target)= 4 x $10^{-7}$

$P_\pi$(>700ns)= 10 x $10^{-18}$

# MECO

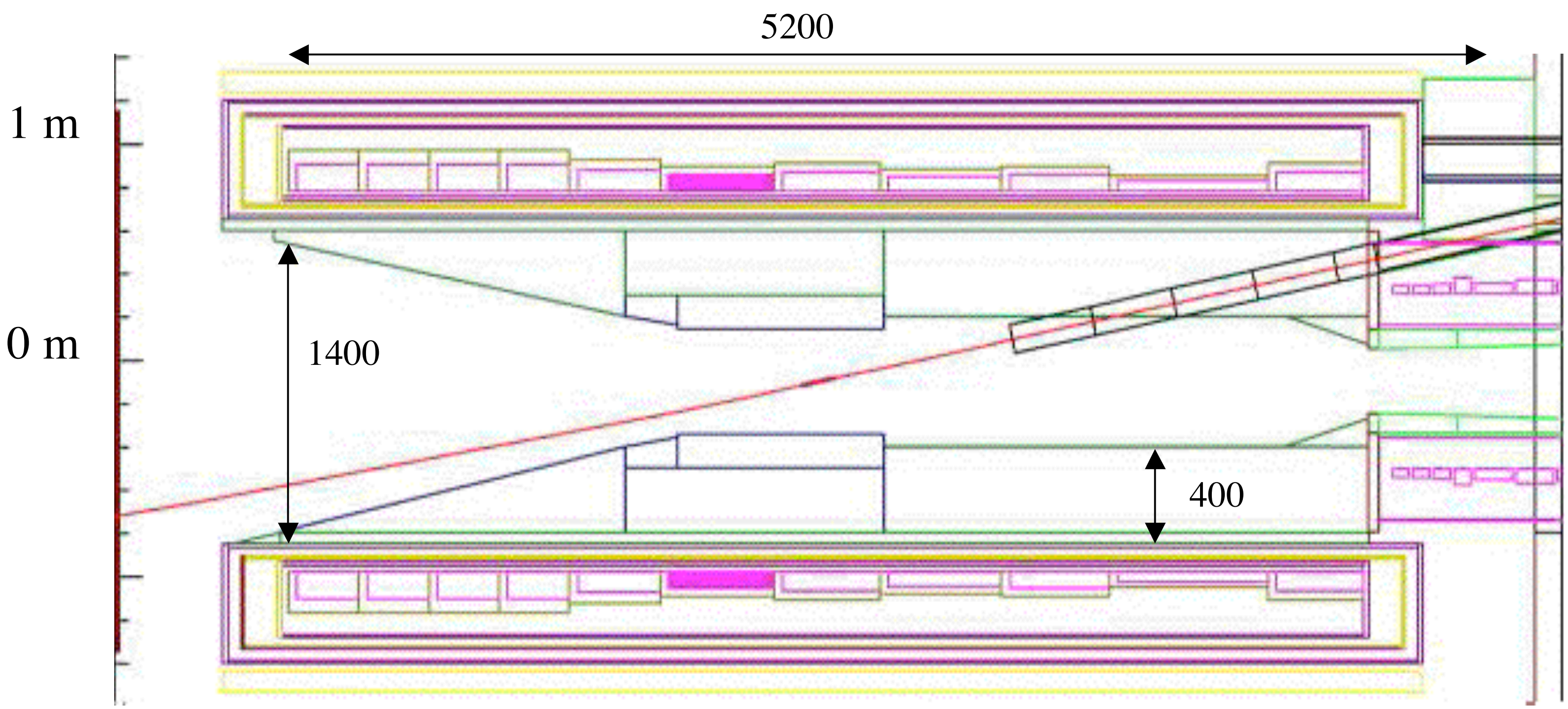


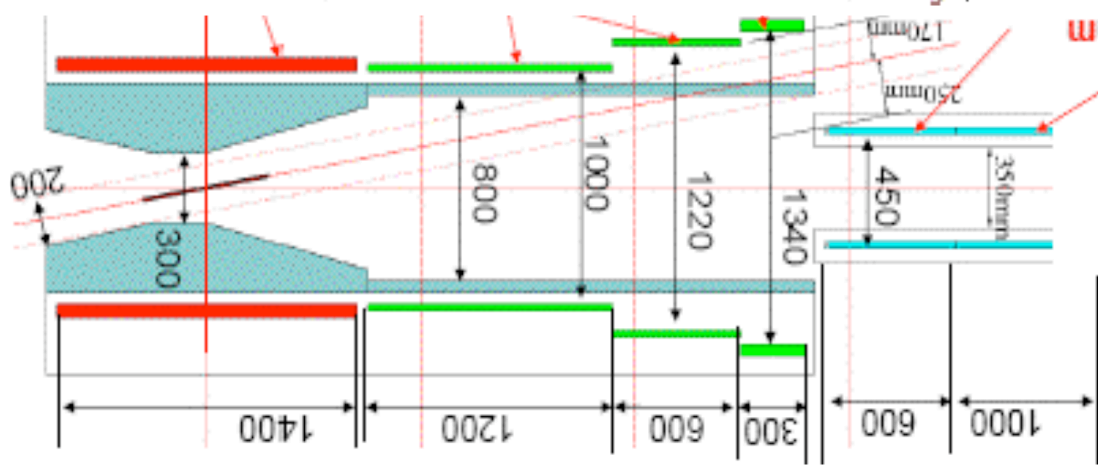

COMET

# Consider a Reduced Length Production Solenoid (~5m to ~3.5m)

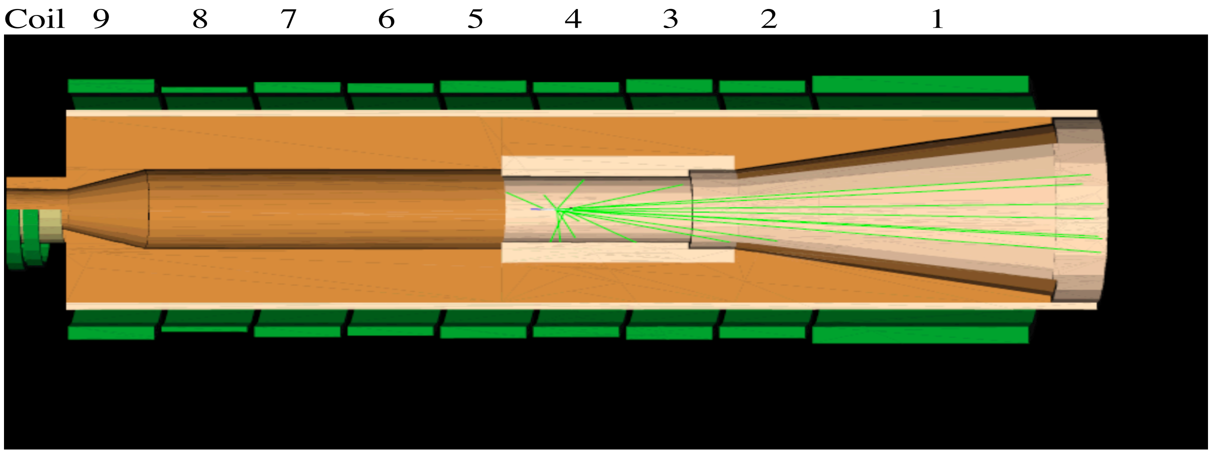


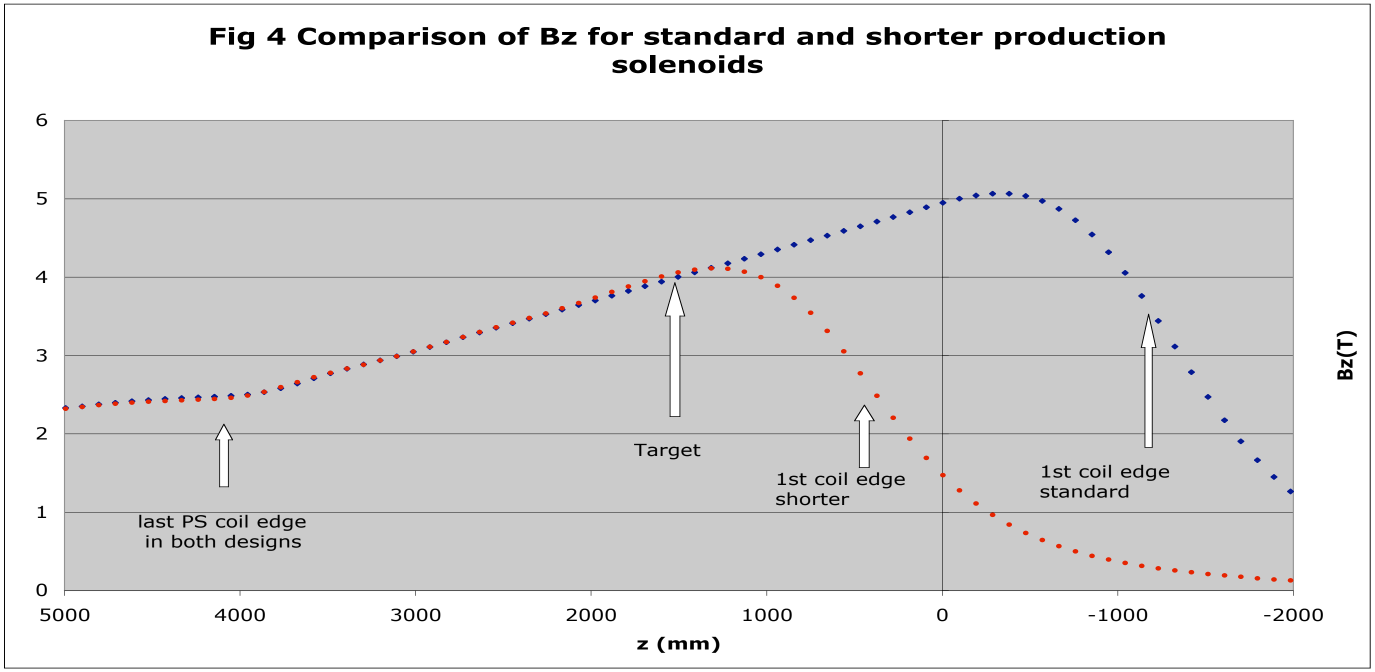

# Stopped Muon Yield with Reduced Length Production Solenoid

The number of muons **stopping in the stopping target** is given below for the standard MECO production solenoid and the shorter version for 1E6 incident protons.

| | QGSP | Armul. et al/MECO | HARP fit |
|---|---|---|---|
| MECO standard PS | 3122 | 2250 | 1280 |
| MECO-shorter PS | 2126 | 1770 | 970 |
| % loss | 32 | 21 | 24 |

Increasing Bmax from 4T to 5T in the shorter version, results in a 13% loss (HARP fit)

# Benefits of Shortening Production Solenoid

M. Lamm slide

- Lower Cost
- Reduced number of coils
- Reduced amount of superconductor/stabilizer
- Less stored energy
- More coil temp margin (indirect cooling possible)
- “2 coil” more like Detector Solenoid: might be easier to spec to vendors

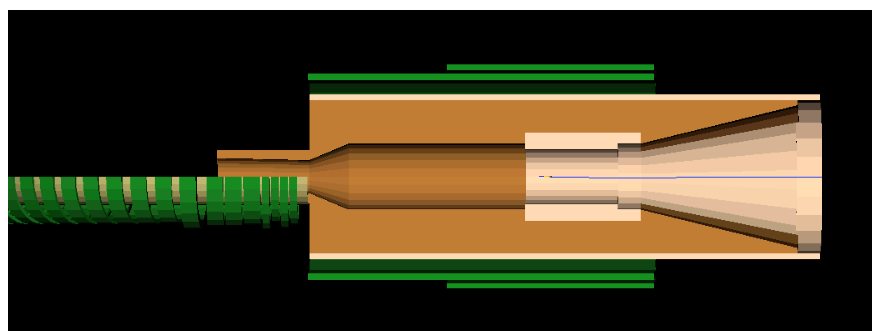

# Transport Solenoid Study Issues

- Simplify # of coil types by relaxing field specs?
  - Review gradient requirements, late particles
- Do we need corrector coils?
- How do we run positives? (rotate collimator/polarity)
- Revisit TSu/TSd interface, pbar window warm section
- Coil Fabrication Technology

# Brief Summary of Fermilab Technical Division Solenoid Studies

- Debriefing and CDR update from General Atomics- contractor for MECO solenoids design

- US/Japan Agreement-Goal to develop technology for Aluminum Stabilized NbTi conductor for Production Solenoid

- Production Solenoid Studies
  - Cost/Performance/Reliabilty/Ease of construction/Temperature margin/Quench & mechanical analysis
  - Shorter Version with 2-coils vs MECO

- Transport Solenoid- alignment tolerance studies

# Summary

- Reproduced many MECO results
- Production Solenoid studied in detail
  - HARP data important, working to incorporate
  - A reduced length PS (à la COMET) attractive
- Transport Solenoid studies starting
- Fermilab Technical Division has made much progress on magnets

# Backup Slides

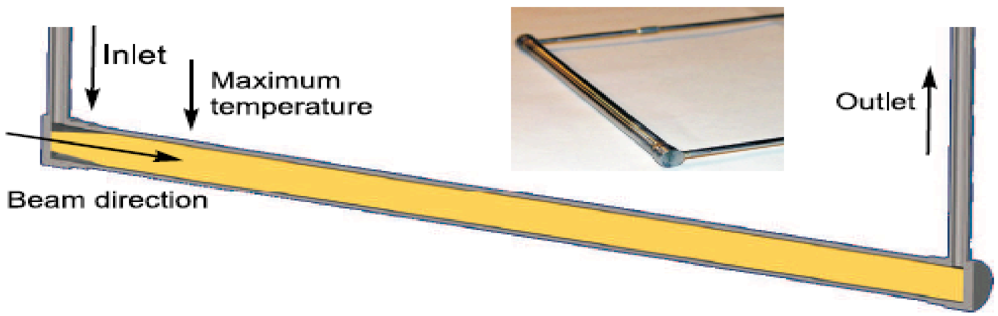


*Figure 7.8: Cross-sectional view of current target cooling design. In our design, the beam strikes a gold target end-on from the left. The target shell, end caps, and inlet & outlet pipes are made of titanium. The target has a slight taper at the inlet which helps reduce the operating pressure; the coolant channel then narrows to 0.3 mm.*

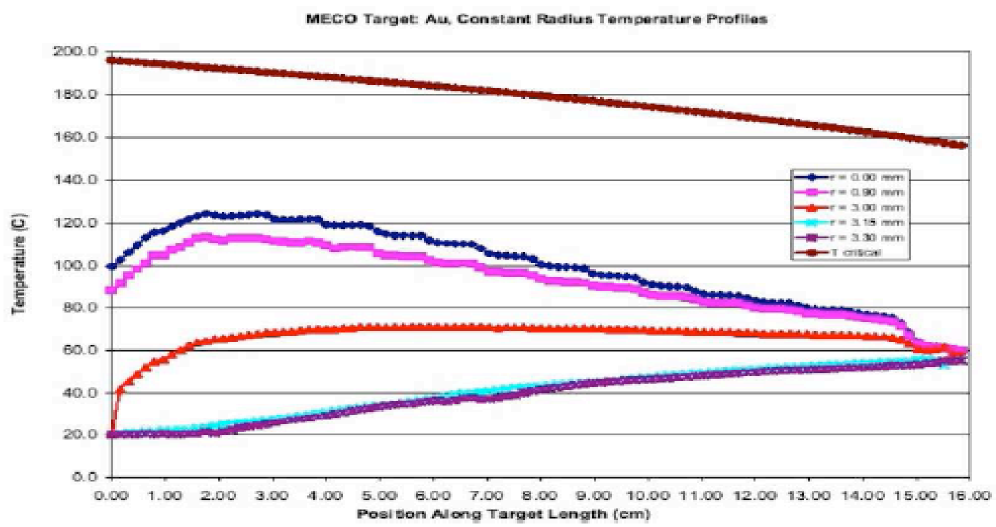


*Figure 7.9: Target and coolant temperature at fixed radii as a function of position along the length. Our chief calculation tool has been CFDesign, a heat and mass transfer program designed for solving complex engineering problems. The results shown here are for a worst-case scenario, steady state heating, with power distribution shown in Fig. 7.7 and 9500 Watts total instantaneous power. Flow rate is 1 gallon per minute.*

# MARS PS coil energy deposition from MARS compared to MECO/GEANT3

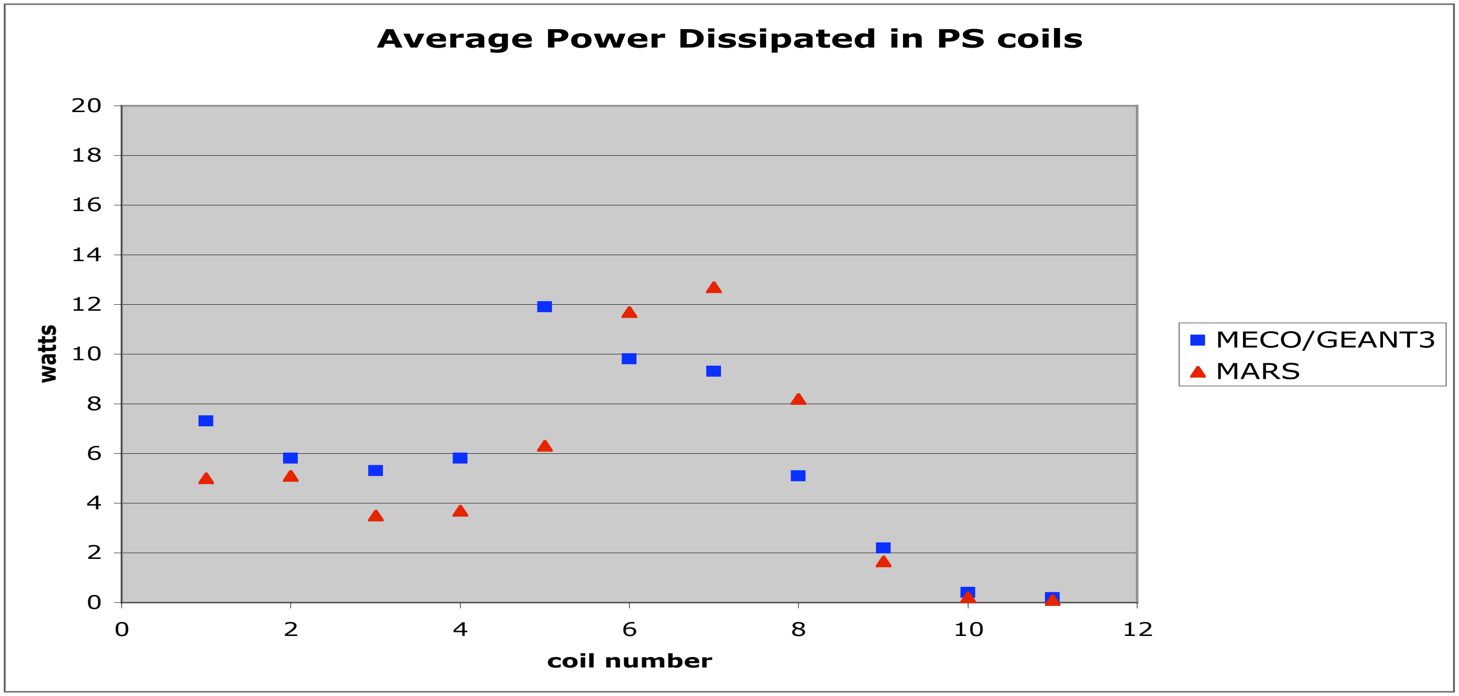


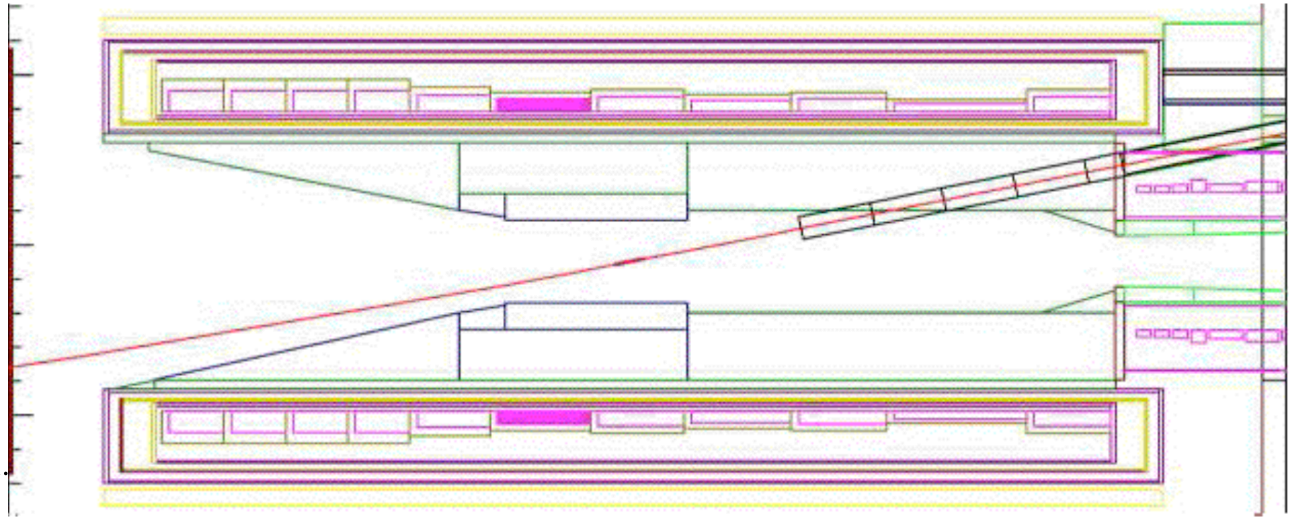

# MECO target optimization

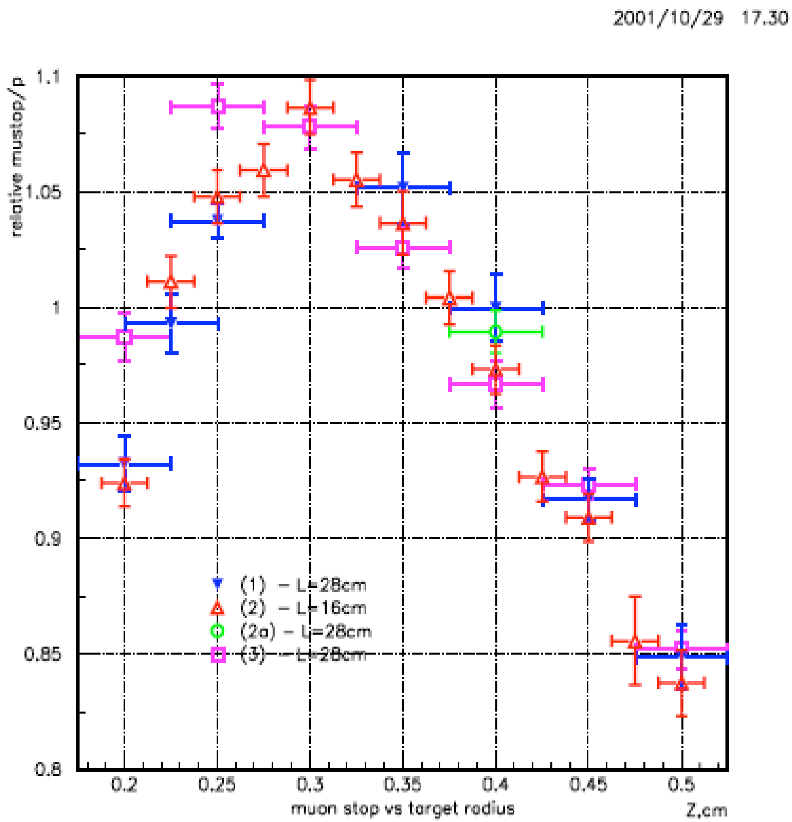


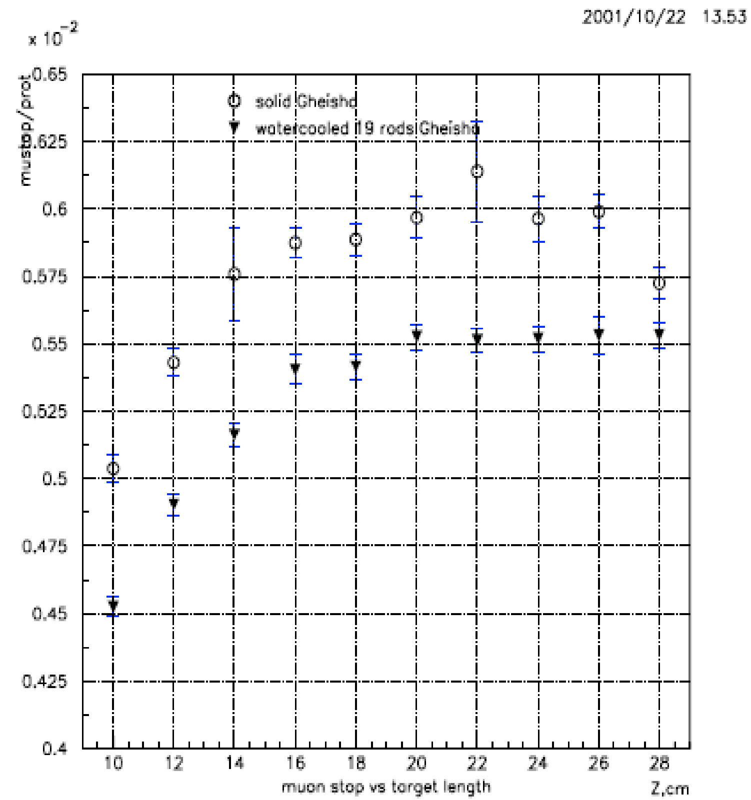

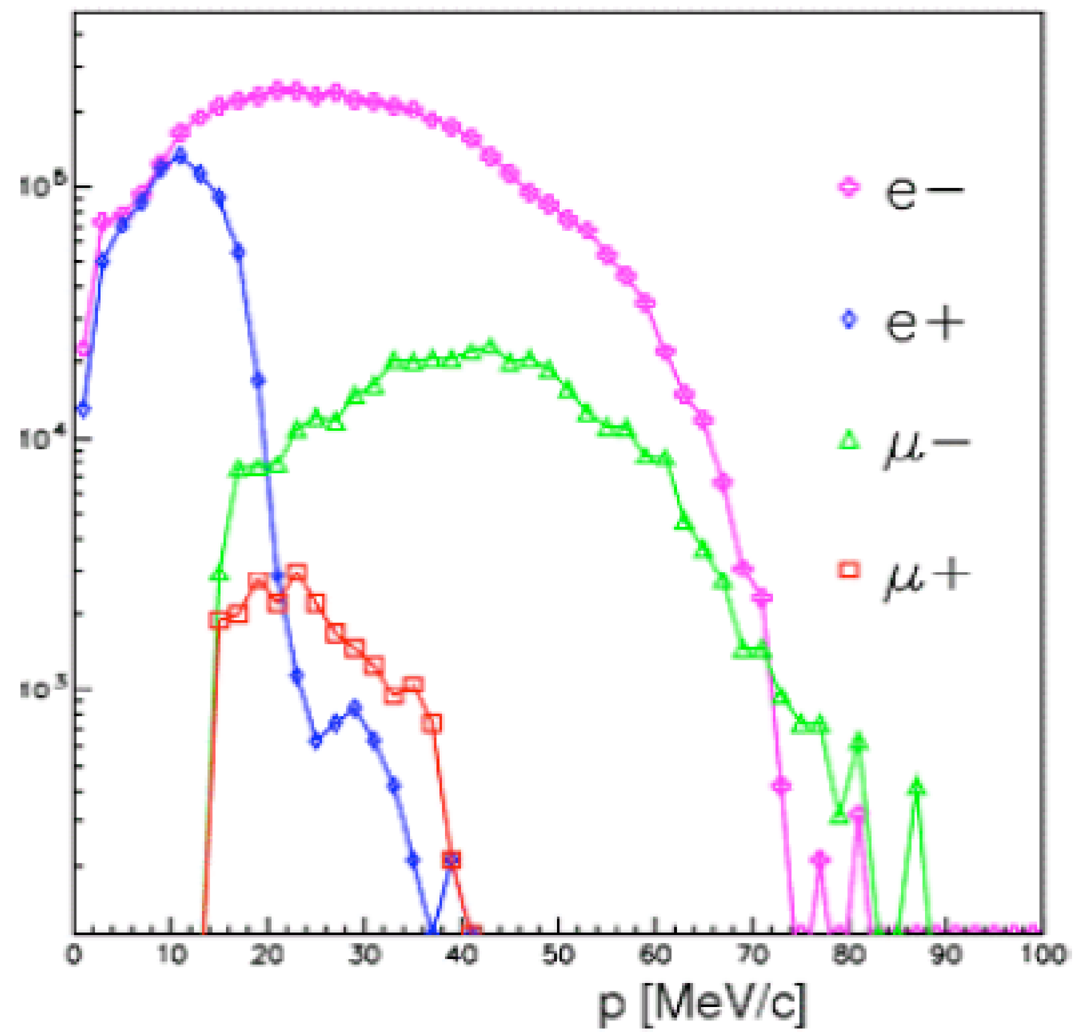
$10^5$
$10^4$
$10^3$
0
10
20
30
40
50
60
70
80
90
100
p [MeV/c]
e−
e+
μ−
μ+

# FANCY fit

- Pion yield was measured by FANCY spectrometer at KEK for p Al at 3 GeV/c and p Al, p Pb at 4 GeV/c.
- Pion kinetic energies were from 100 to 850 MeV, angles - from 36 to 90 degrees.
- Each data set has been fitted by two-fireball model

  (6 parameters, with clear A-dependence of each fireball)

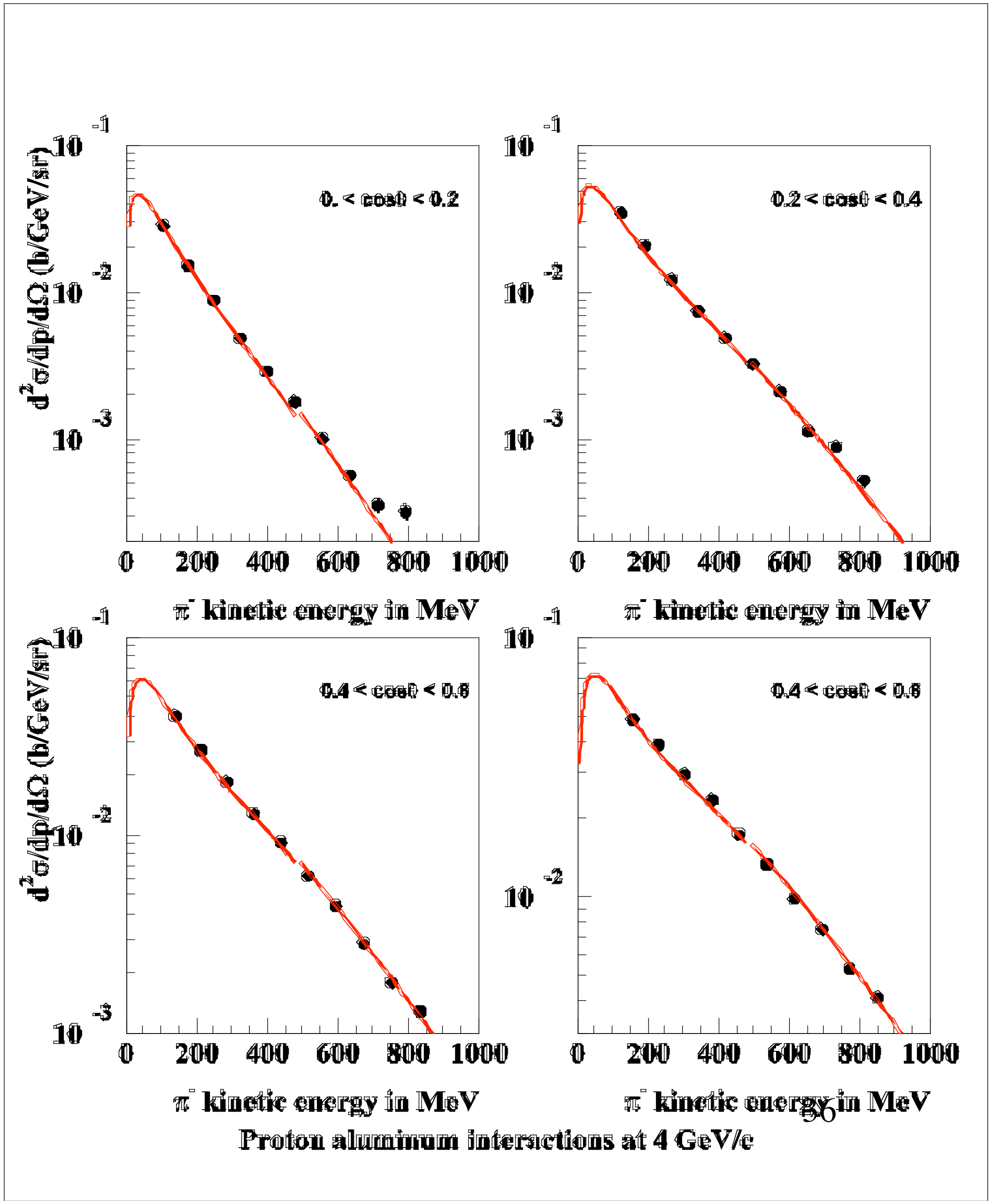

Eur. Phys. J. C (2009) 61: 237–246
DOI 10.1140/epjc/s10052-009-1023-1

THE EUROPEAN PHYSICAL JOURNAL C

Regular Article - Experimental Physics

# GEANT4 simulation of hadronic interactions at 8–10 GeV/c: response to the HARP-CDP group

**V. Uzhinsky[1,2,6,a], J. Apostolakis[2], G. Folger[2], V.N. Ivanchenko[2,3], M.V. Kossov[2,4], D.H. Wright[5]**

**Fig. 1** Two-dimensional distribution of $\pi^+$ mesons in the four-body final state generated by 8 GeV/c pp-interactions before (**a**) and after (**b**) the bug fix

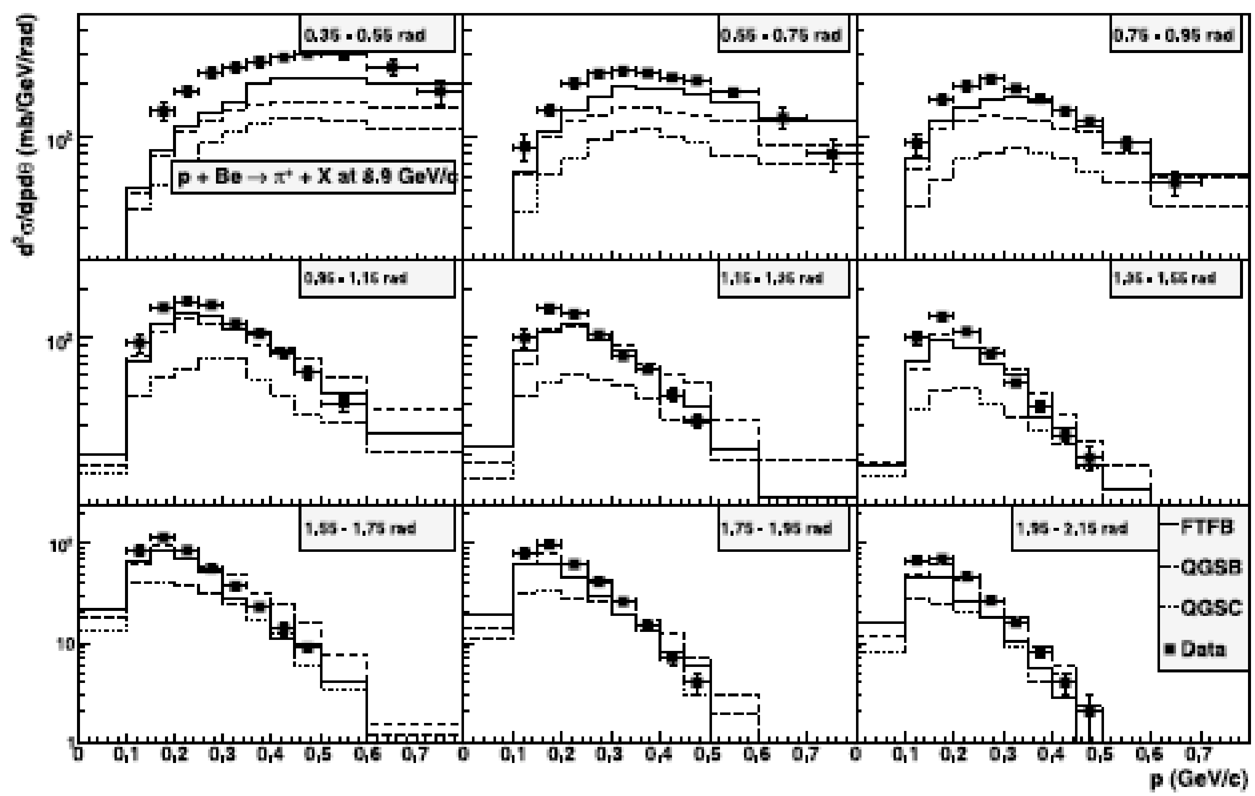




**Fig. 2** Comparison of the experimental data [23, 24] and the string model calculations. FTFB and QGSB are the combinations of the high energy models with the binary cascade model (see Sect. 2)

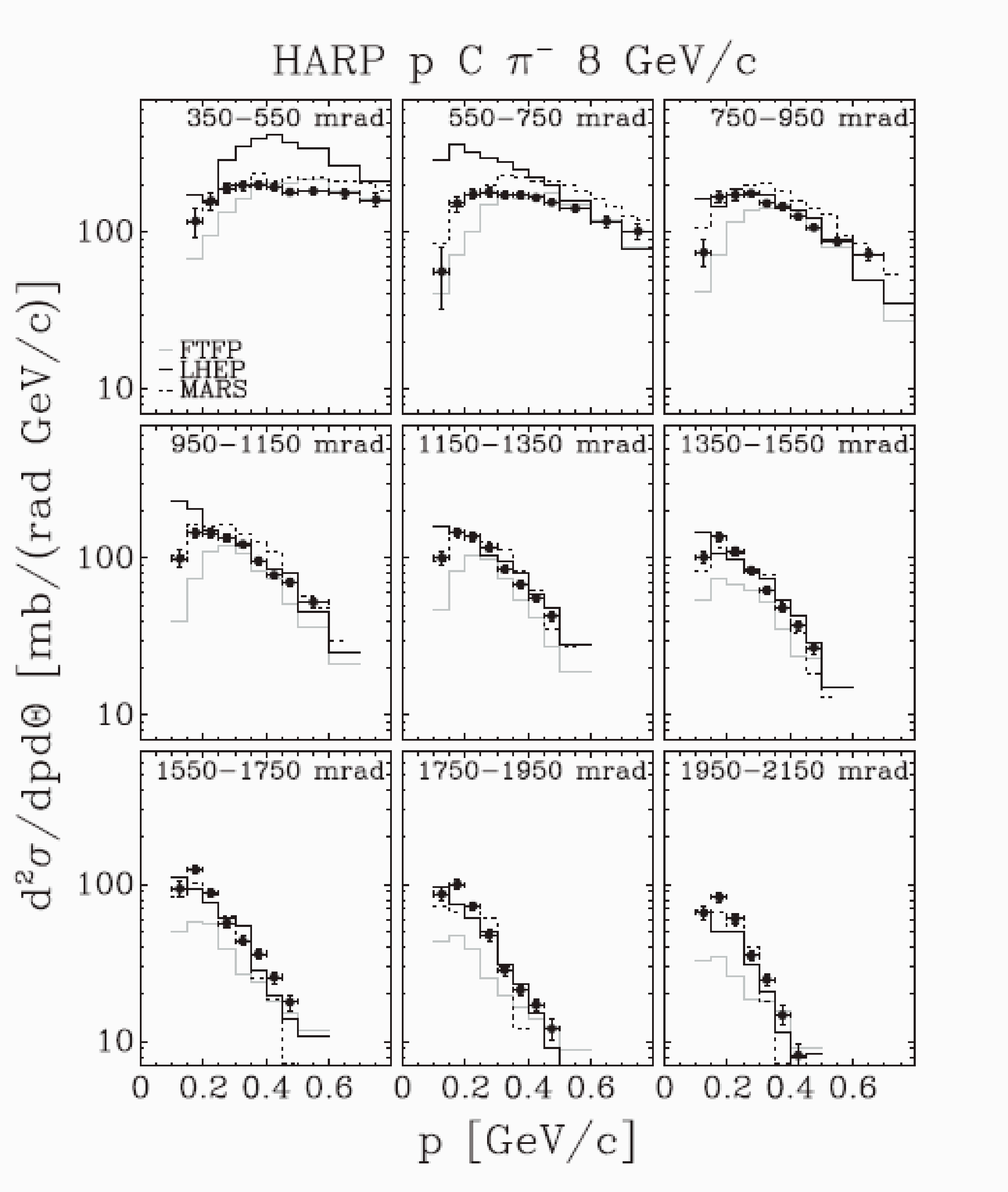


MARS - dash-dotted lines

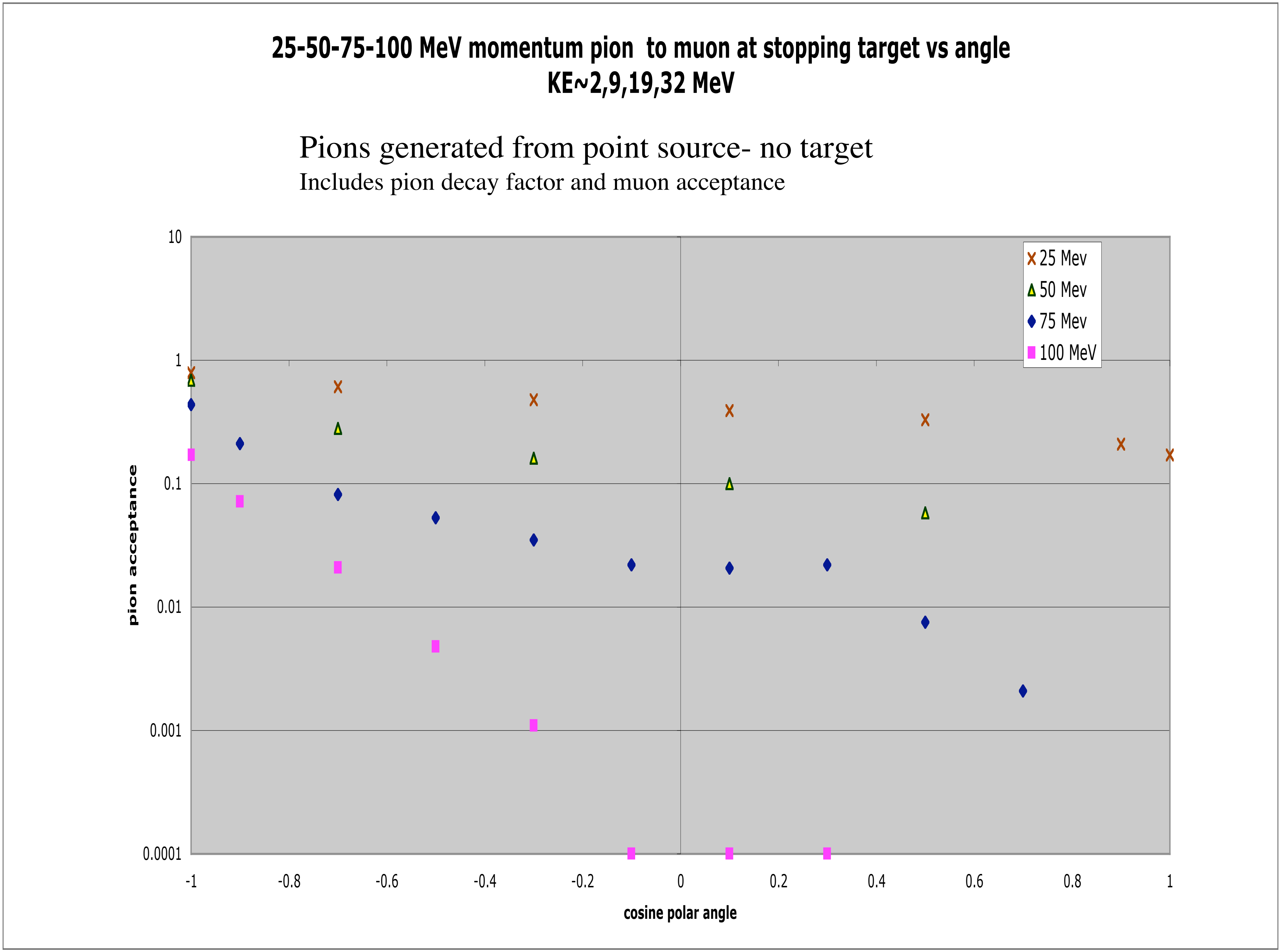
25-50-75-100 MeV momentum pion to muon at stopping target vs angle
KE~2,9,19,32 MeV
Pions generated from point source- no target
Includes pion decay factor and muon acceptance
10
1
0.1
0.01
0.001
0.0001
pion acceptance
-1
-0.8
-0.6
-0.4
-0.2
0
0.2
0.4
0.6
0.8
1
cosine polar angle
25 Mev
50 Mev
75 Mev
100 MeV

# Motion of Charged Particles in a Solenoid with a Gradient Field

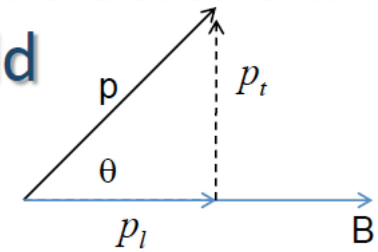


- Solenoid with constant axial field gradient, $G_z$:

$$B_z = B_0 + G_z z \qquad B_r = -\frac{1}{2} G_z r$$

- Low momentum charged particles: helical paths along the field lines.
- $p_t^2/B$=constant, $\rightarrow \; p_t \propto \sqrt{B} \;\; \rightarrow \; p_t = p_t^0 \sqrt{\frac{B_0}{B}}$

**Particles are 'pushed 'in the direction of lower field**

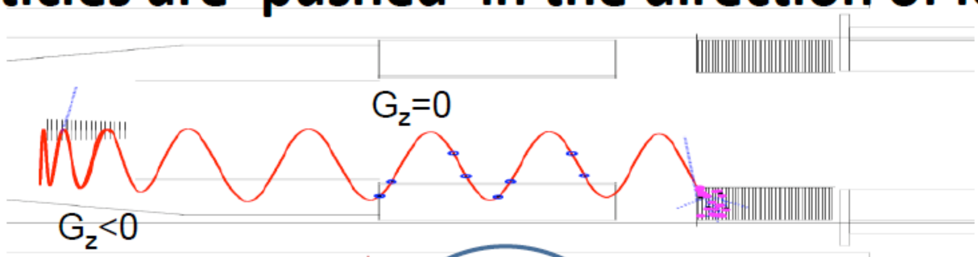


Note that net $q\mathbf{p}_t x\mathbf{B}_r$ points downstream regardless of q (if q flips sign, $\mathbf{p}_t$ reverses direction)

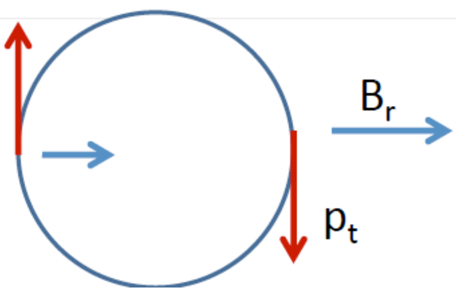


($B_z$ points out of page. Field decreases moving out of page, $G_z$ <0. )

# Solenoid Field Specs

## PS

Axial field on axis:

within 5% of expected value

and $dB_s/ds < -0.02$ T for R<30 cm.

## TS

TS1: First straight section. Field grades linearly 2.5 to 2.4T. Axial ($B_s$) field on axis within 0.5% of expected value. $dB_s/ds < -0.02$T/m for R<15 cm*.

TS2: First toroid. Ripple at outer radius <1% of $B_s$. Field rises from 2.4 T to 2.6 T along inner radius, then returns to 2.4 T. Field on outer radius follows a similar pattern but reduced by 1/R.

* $dB_s/ds < -0.02$T/m relaxed in transition regions from straight to curved sections whenever $|dB_s/dr| > 0.275$ T/m.

T

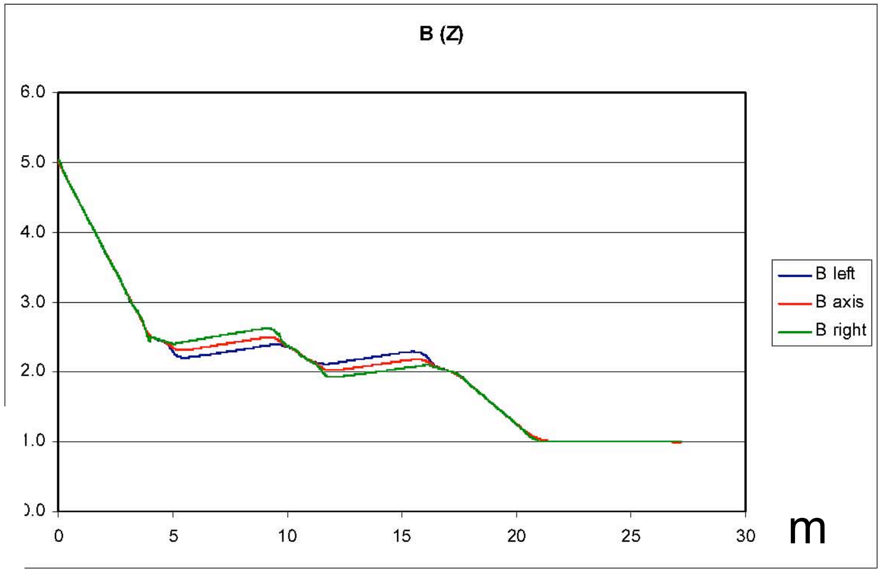


m

Figure 3.4 – Magnetic Field, B(T), along the Paths vs. Z-coordinate (m)

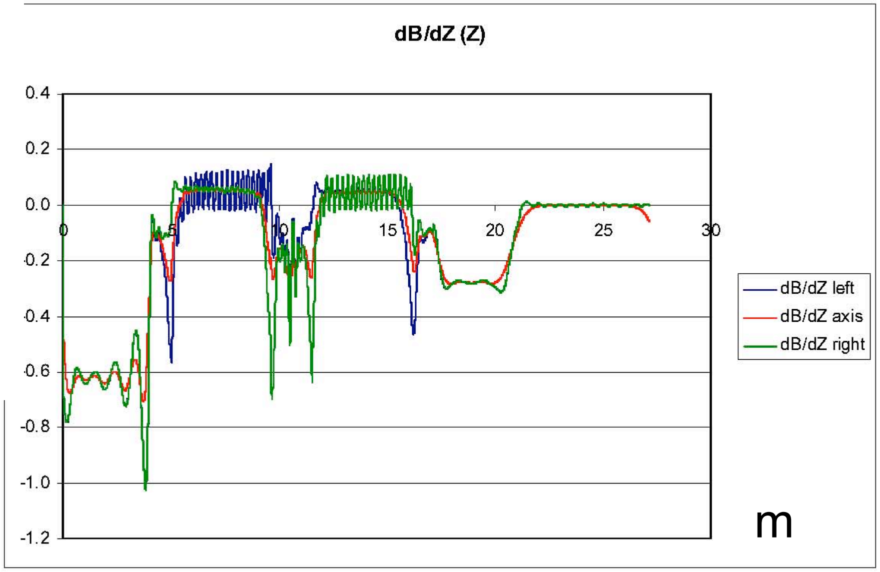


m

Figure 3.5 – Magnetic Field Derivative, dB/dZ(T/m), along the Paths vs. Z-coordinate (m). Relative magnet positions are given by zmin and zmax in Table 3.1.

MECO-doc-167-v1
2001
5T-2T PS
Similar L

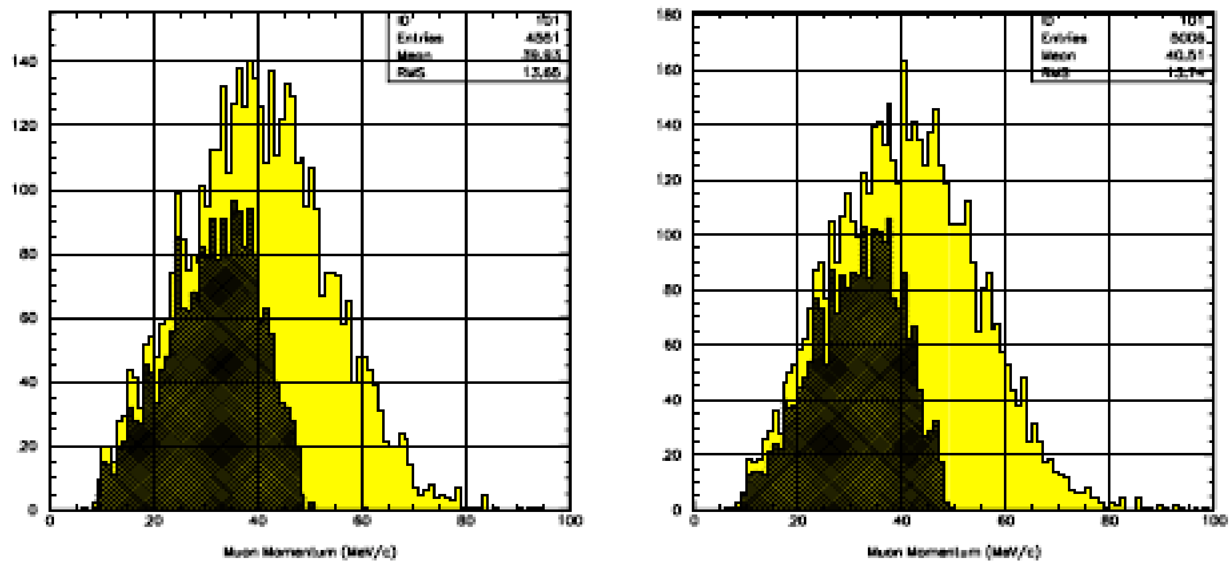


**FIGURE 9.** The momentum distribution for muons entering the detector solenoid (solid) and stopping on the target (hashed) for the thick water-cooled target, maximum magnetic field of 5.0 Tesla, $\pi$ production model I, and bore radii of 20 cm (left) and 30 cm (right).

Stopping Tgt
P dependence

And 0.90 for PS
4.5T to 2T

**TABLE 5.** Muon flux in the detector region from $10^5$ primary generated $\pi^-$ for water-cooled targets (target types 2 and 3) and bore radius 25 cm, using the 2-parameter fit for $T_0$ ($\pi$ production model I).

| Maximum Magnetic Field (Tesla) | Target 2 Muons Entering Detector Region | Target 2 Muons Stopping in Detector Target | Target 3 Muons Entering Detector Region | Target 3 Muons Stopping in Detector Target |
|---|---|---|---|---|
| 5.0 T | 4902 | 2181 | 5655 | 2564 |
| 4.7 T | 4673 | 2167 | 5365 | 2524 |
| 4.5 T | 4434 | 2027 | 4997 | 2423 |



distribution for this calculation, which is very similar to that obtained using pion production model I.

# Time distribution of μ⁻ reaching stopping target

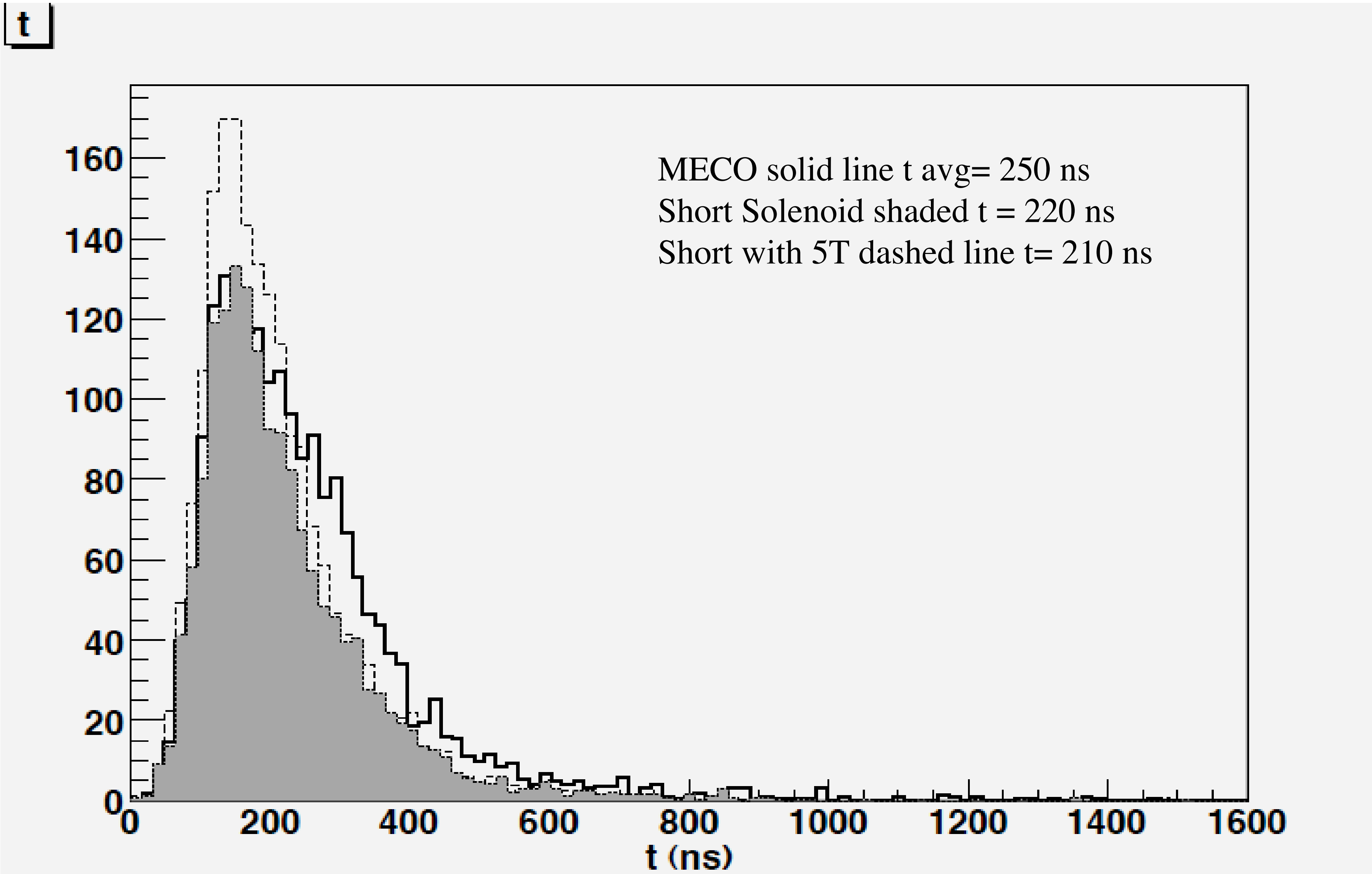

# Transport Solenoid Collimator Dimensions

**Collimator in the First (Highest Field) TSu Straight Section (COL1)**

This consists of a cylindrical outer shell with a conical section removed. It is coaxial with Production Solenoid.

| Position of Center | Inner Radius @ -z end | Inner Radius @ +z end | Outer Radius | Length | Material |
|---|---|---|---|---|---|
| (390.4, 0.0, -345.4) | 15.0 | 17.0 | 24.0 | 100.0 | Cu |

| Position of Center | Outer Radius | Length | Material |
|---|---|---|---|
| (42.5, 0.0, 0.0) | 24.0 | 80.0 | Cu |

**Collimators in Central TSu Straight Section (COL3d)**

The cross-section of this collimator is shown in Figure 3.1. The collimator is coaxial with the x-axis in the Standard MECO Coordinate System.

| Position of Center | Outer Radius | Length | Material |
|---|---|---|---|
| (-42.5, 0.0, 0.0) | 24.0 | 80.0 | Cu |

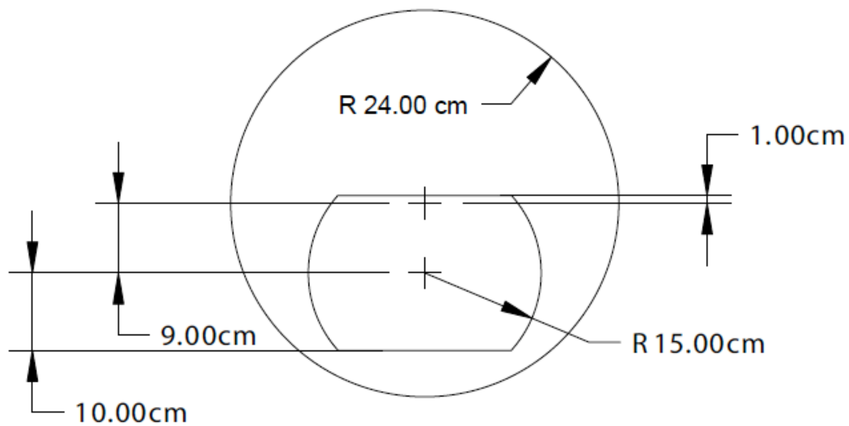


**Figure 3.1 – Cross-sectional view of the central collimators COL3u and COL3d. Note that the outside radius of this collimator is reduced to 24 cm to accommodate a thicker inner cryostat wall relative to the design in the previous version.**

**Collimator in the Last (Lowest Field) TSd Straight Section (COL5)**

This consists of a cylindrical shell that is coaxial with Detector Solenoid.

| Position of Center | Inner Radius | Outer Radius | Length | Material |
|---|---|---|---|---|
| (-390.4, 0.0, 343.0) | 12.8 | 24.0 | 100.0 | Cu |

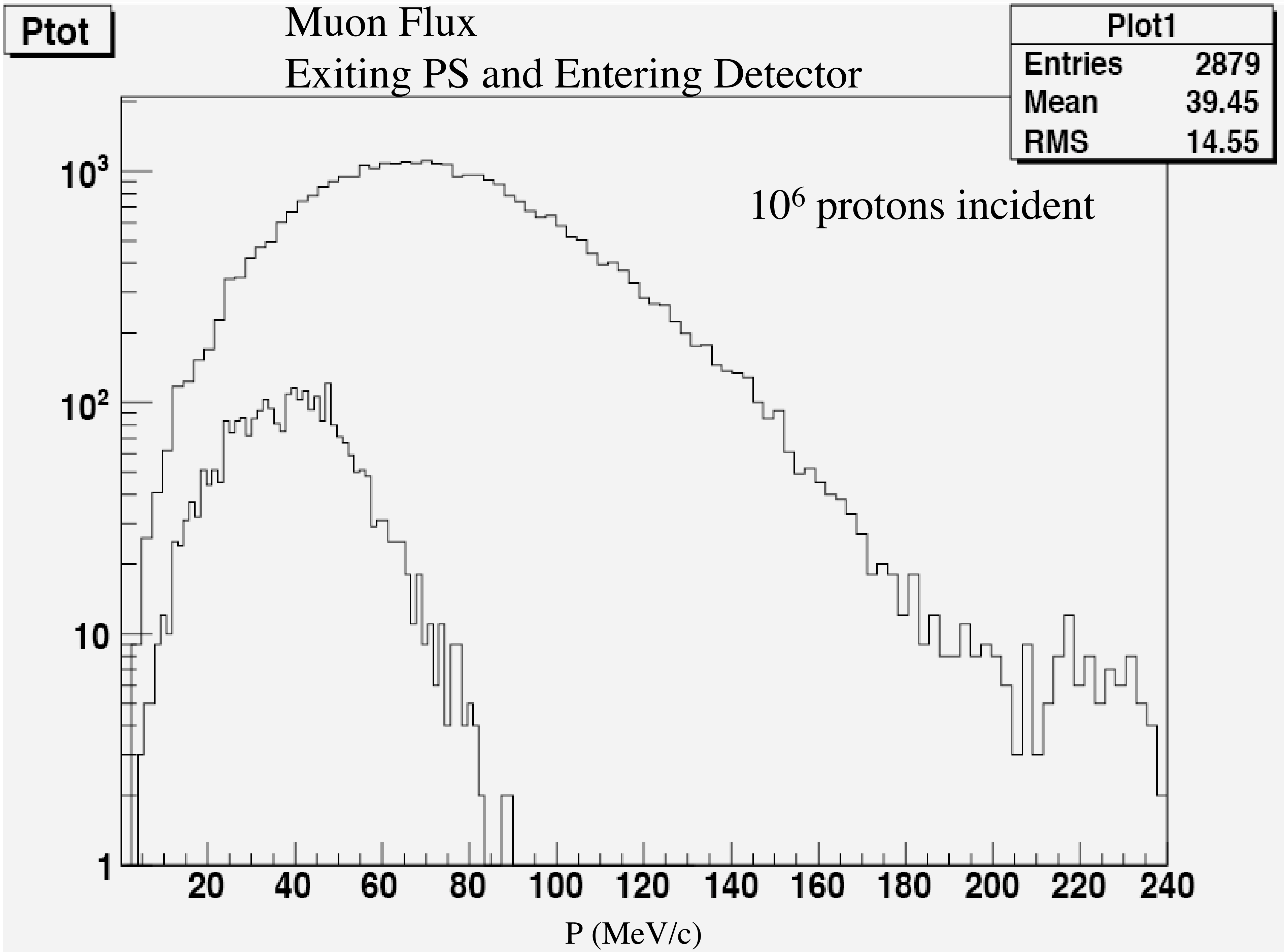
Ptot
Muon Flux
Exiting PS and Entering Detector
Plot1
Entries 2879
Mean 39.45
RMS 14.55
10^6 protons incident
10^3
10^2
10
1
20 40 60 80 100 120 140 160 180 200 220 240
P (MeV/c)

Background Table from Mu2e Proposal

*Table 3.2: The backgrounds from various sources, calculated for the sensitivity given in the previous table, and with scaling as discussed in the text. Backgrounds identified with an asterisk are proportional to the beam extinction and the numbers in the table assume $10^{-9}$ extinction. The number of background events corresponds to a $2\times10^7$ second data collection period, yielding a sensitivity of 4 events for $R_{\mu e} = 10^{-16}$.*

| Source | Events | Comment |
|---|---|---|
| $\mu$ decay in orbit | 0.225 | signal/noise = 20 for $R_{\mu e} = 10^{-16}$ |
| Pattern recognition errors | $< 0.002$ | |
| Radiative $\mu$ capture | $< 0.002$ | |
| Beam electrons* | 0.036 | |
| $\mu$ decay in flight* | $< 0.027$ | without scatter in target |
| $\mu$ decay in flight* | 0.036 | with scatter in target |
| $\pi$ decay in flight* | $< 0.001$ | |
| Radiative $\pi^-$ capture* | 0.063 | from protons during detection time |
| Radiative $\pi^-$ capture | 0.001 | from late arriving $\pi^-$ |
| Anti-proton induced | 0.006 | |
| Cosmic ray induced | 0.016 | assuming $10^{-4}$ CR veto inefficiency |
| Total background | 0.41 | |

in Table 3.2) are proportional to the proton beam extinction and we have assumed a value of $10^{-9}$ for this parameter in calculating the backgrounds shown.